Supporting Information

Radical-Friedel-Crafts Benzylation of Arenes over the Metallic-Basic Bifunctional MoO_2 Surface

Zhuo Li,[a] KaiYi Su,[b] Ting Li,[a] Jinlan Cheng,[a] Bo Jiang, [a] Tingwei Zhang,[a] and Chaofeng Zhang[a]*

[a] College of Light Industry and Food Engineering, Nanjing Forestry University, Nanjing 210037, China

[b] Key Laboratory of Photochemical Conversion and Optoelectronic Materials, Technical Institute of Physics and Chemistry, Chinese Academy of Sciences, Beijing 100190, China

Corresponding Authors: zhangchaofeng@njfu.edu.cn

Contents

1. The crystal structure of the Mo-based catalysts

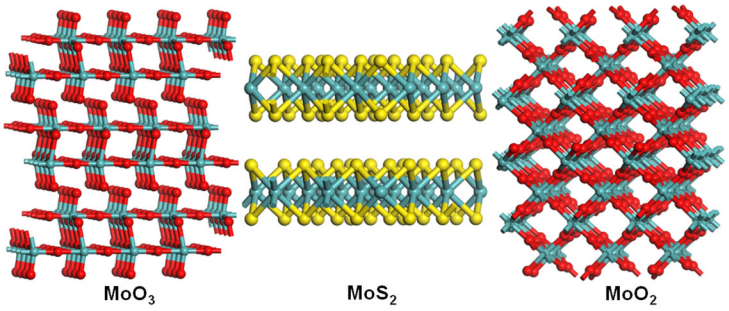

Figure S1. The crystal structure of the Mo-based catalyst

2. TEM images of the as-synthesized MoO_2

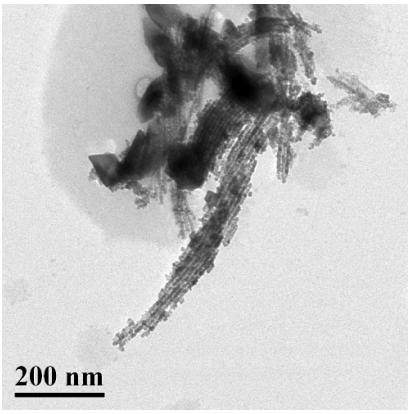

Figure S2. The TEM images of the as-synthesized MoO_2

3. The CO_2-TPD characterization of MoO_2

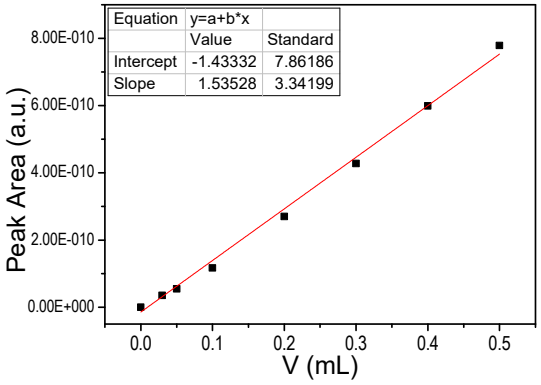

Figure S3. The standard working curve of CO_2 for CO_2-TPD characterization

Characterization procedure: MoO_2 NPs were treated by the H_2 (10 v% in Ar) reduction at 450 °C for 0.5 h, then the cooled MoO_2 NPs were then exposed to the CO_2 atmosphere for 0.5 h at room temperature, with MS line m/z=44 as the typical signal of CO_2 and referring to the standard working curve of CO_2.

4. The BET characterization of MoO_2 catalysts

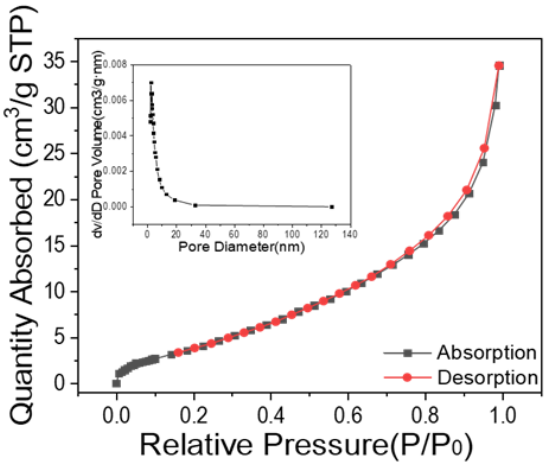

Figure S4. BET data analysis of commercial MoO_2

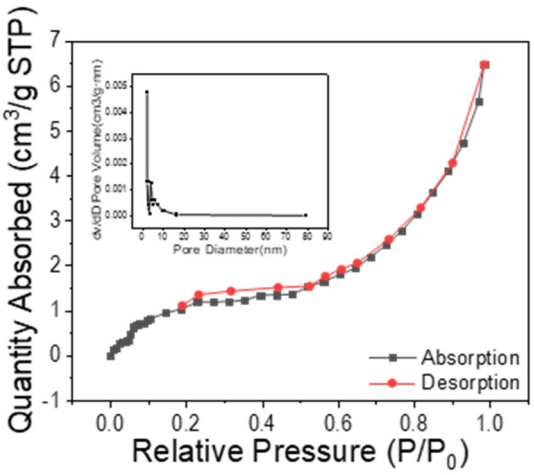

Figure S5. BET data analysis of MoO_2 synthesized by the template method

5. Catalyst screen for the catalytic benzylation of the PX with DBE

Table S1. Catalytic Benzylation of the PX with DBE over various catalysts[a]

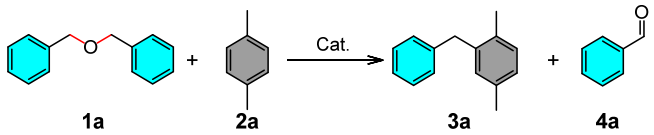

Entry	Catalyst	1a Conv.(%)	Yield (%)		Entry	Catalyst	1a Conv.(%)	Yield (%)	
			3a	4a				3a	4a
1	MoO_2	78.9	77.7	0.2		Fe_2O_3	0.5	<0.1	0.3
2	MoO_3	2.3	0.4	1.5		CuO	2.3	<0.1	1.5
3	MoO_x-150[b]	74.3	74.2	<0.1		Cu_2O	2.8	<0.1	1.1
4	MoO_x-520[c]	2.4	2.0	0.1	11	PbO	0.7	<0.1	0.3
5	MoO_2[d]	66.7	66.2	0.3		PrO_2	1.5	<0.1	1.4
6	MoO_2[e]	67.5	67.1	0.2		CdO	2.5	<0.1	1.5
	Al_2O_3	2.1	<0.1	1.2		Ta_2O_5	1.7	<0.1	1.3
	SiO_2	2.1	<0.1	1.8		$FeCl_3$	69.1	69.0	<0.1
	Ga_2O_3	2.7	<0.1	1.4		$AlCl_3$	65.0	64.6	<0.1
7	GeO_2	2.8	<0.1	1.4	12[f]	$SnCl_4$	9.4	9.2	<0.1
	ZrO_2	1.5	0.1	1.4		$NbCl_5$	70.2	70.0	<0.1
	Nb_2O_5	1.7	<0.1	1.4		$MoCl_5$	89.1	87.7	<0.1
	HfO_2	60.8	59.8	1.0	13	TsOH	>99	>99	<0.1
	TiO_2-A	1.6	0.1	1.6		TS-1	1.3	<0.1	1.3
	TiO_2-R	1.5	<0.1	1.4		H-ZSM-5	10.9	9.1	1.3
	V_2O_5	11.3	7.8	1.7	14	H-Beta	1.3	<0.1	1.0
	SnO_2	2.1	<0.1	1.3		SBA-15	<0.1	<0.1	<0.1
8	Sb_2O_3	1.8	<0.1	1.5		MCM-41	40.2	40.1	<0.1
	Sb_2O_5	1.8	<0.1	1.4		Ru/C	<0.1	<0.1	<0.1
	Ta_2O_5	1.7	<0.1	1.3	15	Rh/C	3.0	0.3	0.1
	WO_3	4.7	3.0	1.6		Pd/C	1.2	0.1	0.6
	MgO	<0.1	<0.1	<0.1		Pt/C	1.2	<0.1	0.6
	Sc_2O_3	1.3	<0.1	1.1		Pd/CeO_2	<0.1	<0.1	<0.1
9	Y_2O_3	2.0	<0.1	1.4	16	Pd/MgO	<0.1	<0.1	<0.1
	La_2O_3	1.7	<0.1	1.2		Pd/ZnO	<0.1	<0.1	<0.1
	Eu_2O_3	1.3	<0.1	1.0		2H-MoS_2	12.0	10.7	0.9
	Cr_2O_3	4.9	<0.1	0.9		MoC_2	72.1	71.8	0.2
	MnO_2	1.3	<0.1	0.6	17	MoP	<0.1	<0.1	<0.1
	Mn_3O_4	2.2	<0.1	1.0		MoB	9.8	9.6	0.2
	Co_3O_4	1.2	0.1	0.3		$MoSi_2$	5.8	1.2	4.7
10	NiO	2.2	<0.1	0.9		$MoSe_2$	0.4	0.4	<0.1
	ZnO	2.0	0.1	1.2	18	MoO_2[g]	73.9	70.5	<0.1
	In_2O_3	1.9	<0.1	0.8	19	MoO_2[h]	<0.1	<0.1	<0.1
	CeO_2	1.7	<0.1	1.4	20	MoO_2[i]	>99	99	<0.1
	Bi_2O_3	1.6	<0.1	1.1					
	Cr_2O_3	4.9	<0.1	0.9					

(a)Reaction conditions: Catalyst 100 mg, dibenzyl ether (DBE) 0.1 mmol, PX 2.0 mL, Ar 1 atm, 140 °C, 10 min; symbol --- means no additive or no product; (b) the catalyst is 150 °C-oxidized MoO_2; (c) the catalyst was MoO_2 treated in the air flow at 520 °C; (d) reaction atmosphere is O_2; (e) reaction atmosphere is Air; (f) catalyst is 2 mol%; (g) Additive is BHT; (h) additive is TEMPO; (i) reaction time is 1 h.

6. Optimization of reaction conditions

6.1 The effect of reaction temperature

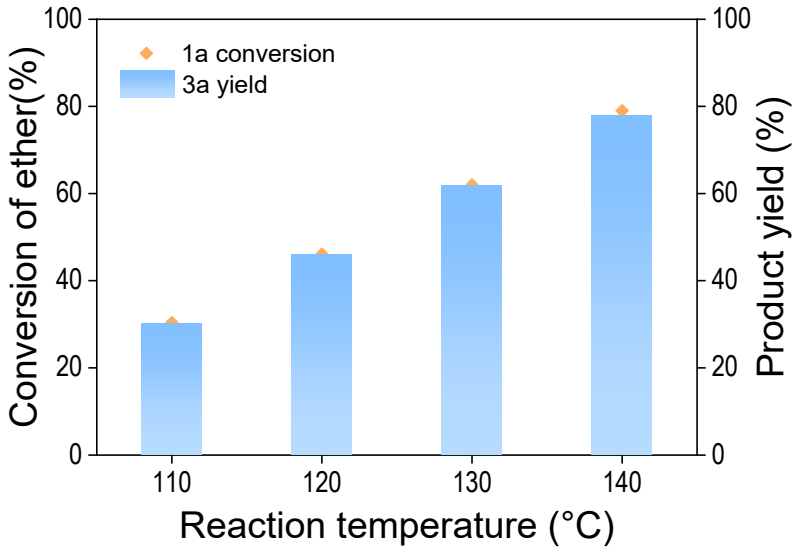

Figure S6. The effect of reaction temperature on **1a** conversion and **3a** yield. Reaction conditions: MoO_2 100 mg, dibenzyl ether 0.1 mmol, PX 2.0 mL, 10 min, Ar 1 atm.

To calculate the apparent activation energy, the initial rate of the reaction was measured as a function of temperature (80, 90, 100, and 110 °C). In a typical reaction, in the glove box under the Ar atmosphere, dibenzyl ether (0.1 mmol) and MoO_2 (100 mg) were added in p-xylene (2.0 mL) in a 15 mL tube equipped with a Teflon stopcock. The reaction was stirred in an oil bath preset at a preset temperature for 10 min. Then, the tube was removed from the oil bath and immediately cooled in an ice-water bath. After the tube was open to the air, the dodecane (36.9 mg) as the standard substance was added to the reaction mixture. After the filtration with a Teflon filter membrane, the organic products are analyzed by GC-FID. The slope was used to calculate the apparent activation energy Ea=43.4 $kJ \cdot mol^{-1}$ according the Arrhenius Equation:

6.2 The effect of reaction time

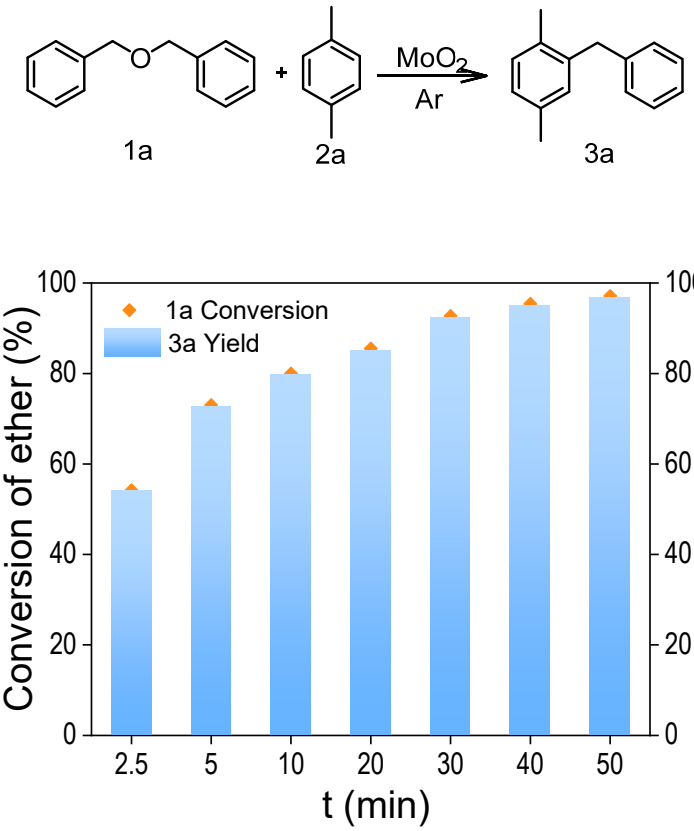

Figure S7. The effect of reaction time on **1a** conversion and **3a** yield. Reaction conditions: MoO_2 100 mg, dibenzyl ether 0.1 mmol, PX 2.0 mL, 140 °C, Ar 1 atm.

7.Hot-filtration test

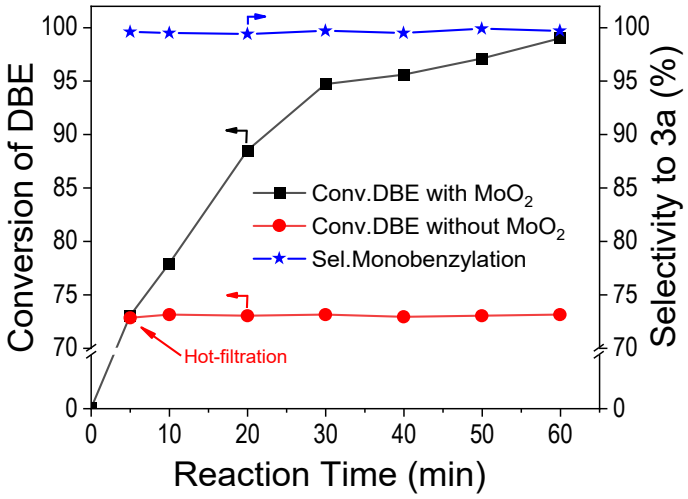

Figure S8. Benzylation of PX with DBE over MoO_2.Reaction conditions: MoO_2 100 mg, dibenzyl ether 0.1 mmol, PX 2.0 mL, 140 °C, Ar 1 atm.

To identify whether the MoO_2 catalyst is a heterogeneous catalyst, hot filtration testing was performed. When the reaction time is 5 minutes, the MoO_2 catalyst should be immediately filtered out of the catalytic reaction system while it is still hot. The reaction should then continue for 120 minutes under the same reaction conditions, and a small amount of the reaction mixture was taken at regular intervals during the reaction for quantitative analysis. The resulting experimental results are shown in Figure S8, no further reaction of the filtrate was detected after hot filtration, indicating that there was barely leached out of the active species and that MoO_2 catalyst did act as a heterogeneous catalyst.

8. Reuse test of MoO_2 and XRD characterization

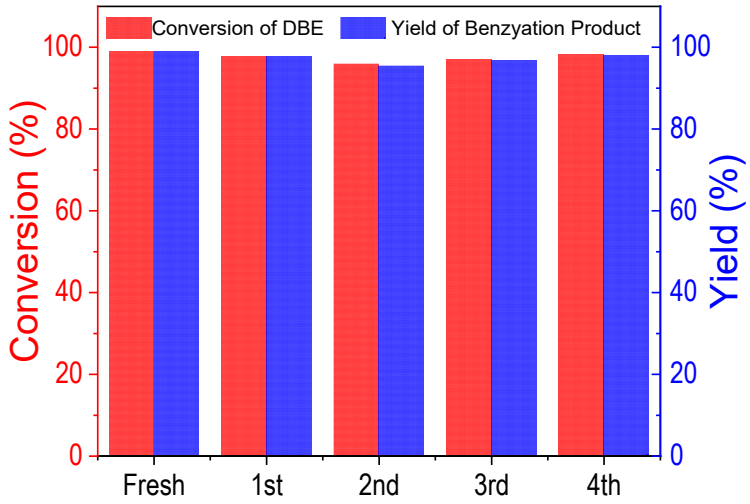

Figure S9. The reusability of MoO_2 in the benzylation of PX with DBE. Reaction conditions: MoO_2 100 mg, DBE 0.1 mmol, PX 2.0 mL, Ar, 140 °C, 1 h. The recycled catalyst was reused without further fresh catalyst addition after separation from the previous reaction mixture and simple vacuum drying.

In the context of catalysts, the stability of their cycling reaction performance represents a crucial evaluation criterion for assessing their catalytic efficacy. In the case of heterogeneous MoO_2 catalysts, the separated MoO_2 could be recycled on four occasions without any change in activity following ethanol washing and vacuum drying. The results of the experiments are presented in **Figure S9**. After recycling, the MoO_2 catalysts demonstrated consistent catalytic performance, with only a slight decline in substrate conversion, and the selectivity of the benzylation products remained above 99%. The slight conversion decrease can be attributed to the sensitivity of the MoO_2 surface to the air after several times of exposure during the catalyst recycling and drying. The aforementioned experimental results demonstrate that the MoO_2 catalyst exhibits remarkable reusability.

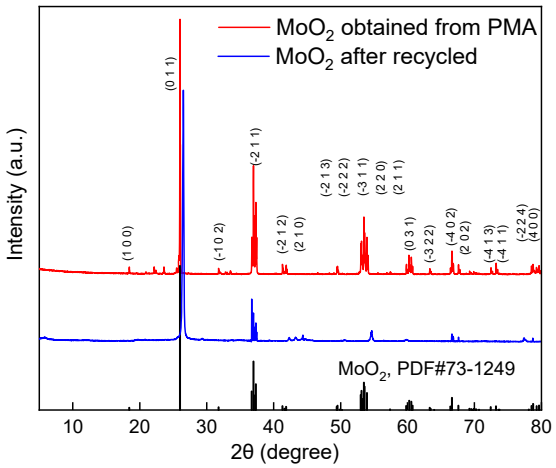

Figure S10. XRD characterization of catalysts before and after cyclic reactions.

Analysis of the XRD characterization results showed that there was no significant difference in the XRD patterns of molybdenum dioxide after four cyclic reactions. This indicates that the cyclic reaction process did not cause significant changes in the bulk structure or crystallinity of molybdenum dioxide, and the weakening of some peaks may be related to the slight oxidation of the catalyst.

9. The benzylation reactions between styrene and DBE

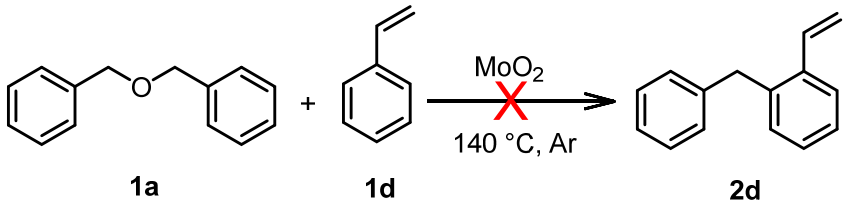

Figure S11. Polymerization of styrene and dibenzyl ether catalyzed by MoO_2. Reaction conditions: MoO_2 100 mg, dibenzyl ether 0.1 mmol, dodecane 2.0 mL, 140 °C, Ar 1 atm.

The MoO_2-catalyzed benzylation between styrene and benzyl ether presented a distinctive phenomenon that deviates from the conventional reaction. As illustrated in **Figure S11**, the rapid polymerization of the reactants formed a solid colloid under the specified reaction conditions at 140 °C. It is postulated that the styrene molecule may be attacked by the radicals thermally decomposed from DBE, which can initiate the polymerization reaction of a high-viscosity solution or melt. The high viscosity colloid adheres to the inner wall of the reaction vessel and the rotor of the stirrer, thereby preventing further stirring.

10. Hammett study

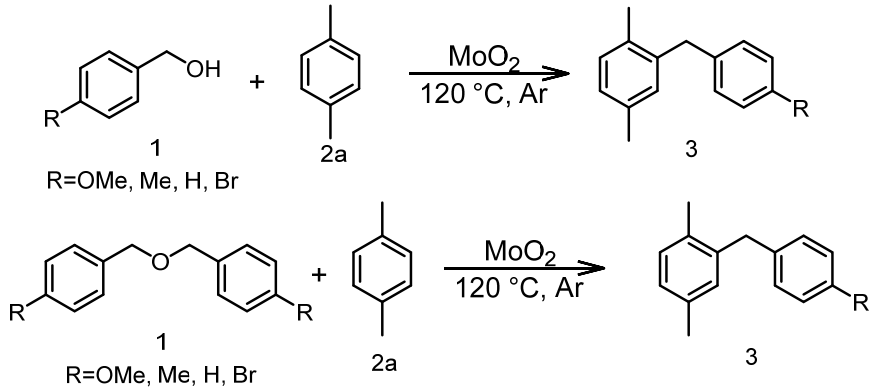

Scheme S1. Hammett study

In a glove box under the Ar atmosphere, para-substituted benzyl alcohols (1.0 mmol) or para-substituted dibenzyl ether (0.1 mmol), and MoO_2 (100 mg) were added in p-xylene (2.0 mL) in a 15 mL tube equipped with a Teflon stopcock. The reaction was stirred in an oil bath preset at 120 °C for 3 min (10 min for para-substituted dibenzyl ether). Then, the tube was taken out of the oil bath and immediately cooled in an ice-water bath. After the tube was opened to air, the Dodecane (0.01 mmol) as the standard substance was added into the reaction mixture. After the filtration with a Teflon filter membrane, the organic products are analyzed by NMR. The conversion was determined by NMR by measuring the appearance of the product.

11. EPR measurements of the intermediate of benzylation reaction

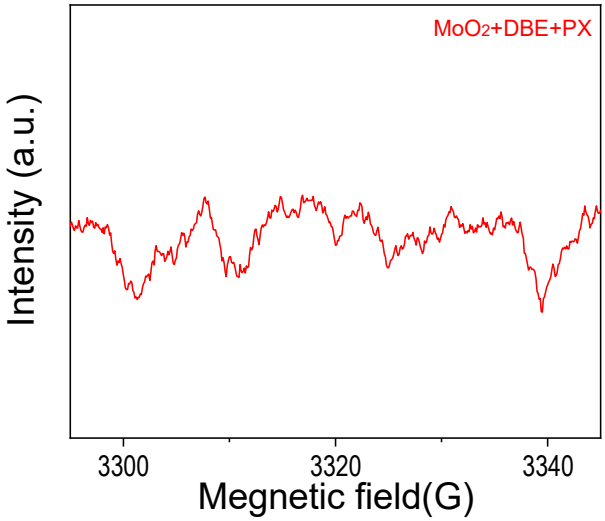

Figure S12. EPR measurements. Reaction conditions: MoO_2 200 mg and DBE 0.5 mmol, PX 2.0 mL, 140 °C, Ar atmosphere. After 5 minutes of reaction, 0.25 mmol DMPO was injected into the system and the tube was immediately cooled down by liquid nitrogen. After the filtration with a Teflon filter membrane, the sample was transferred to a glass capillary and placed in a sealed glass tube under an Ar atmosphere for the EPR test.

12. Radical trap experiment with TEMP

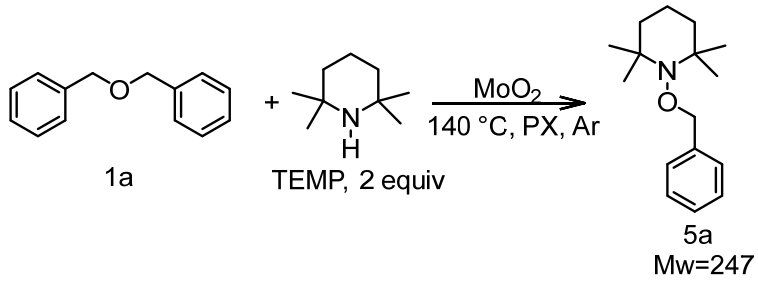

Scheme S2. Radical trap experiment with TEMP

In a glove box under the Ar atmosphere, dibenzyl ether (0.2 mmol), and MoO_2 (100 mg) were added in p-xylene (2.0 mL) in a 15 mL tube equipped with a Teflon stopcock. The reaction was stirred in an oil bath preset at 140 °C for 2 min. Then, 2,2,6,6-tetramethylpiperidine (TEMP, 1.0 mmol) was added under Argon atmosphere and the reaction was cooled down. After the filtration with a Teflon filter membrane, the organic products are analyzed by GC-MS (GC: Shimadzu 2030AM, MS: Shimadzu, QP2020NX). The mass spectrum of **5a** is shown in **Figure S13** with an m/z = 247.

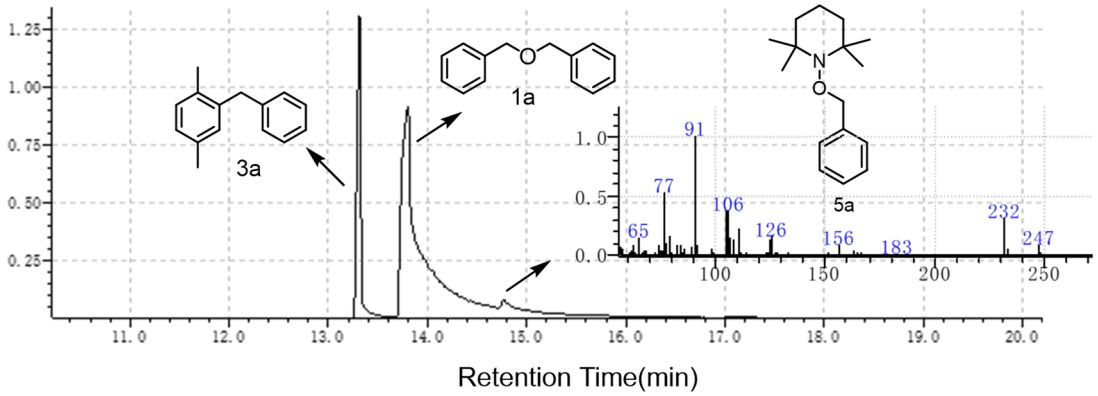

Figure S13. The GC-MS pattern of the radical trap experiment with TEMP

12. Self-decomposition of DBE in Dodecane

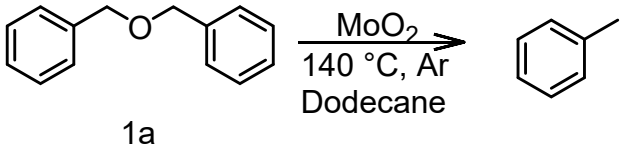

1a

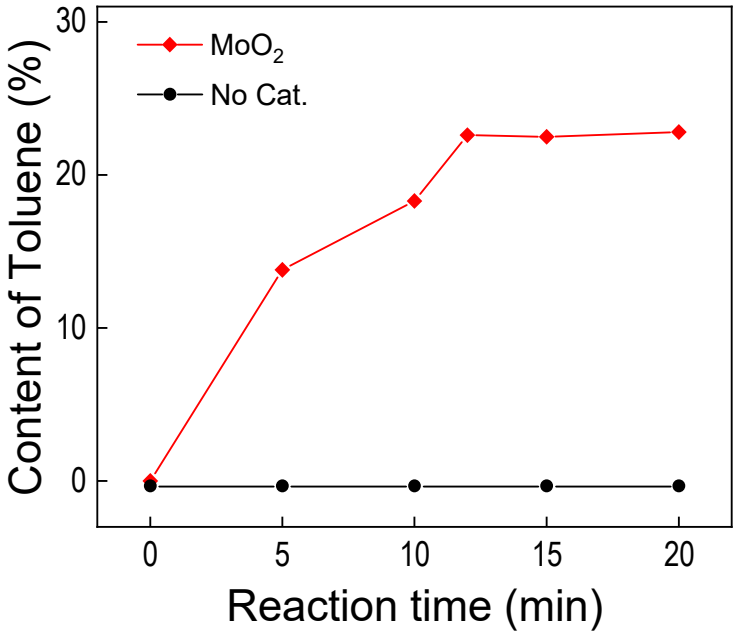

Figure S14. Content of toluene versus reaction time of self-decomposition of DBE in the absence or presence of MoO_2. Reaction conditions: MoO_2 100 mg, dibenzyl ether 0.1 mmol, dodecane 2.0 mL, 140 °C, Ar 1 atm.

The experiment procedure was similar to the previous typical reaction, in a 15.0 mL tube equipped with a Teflon stopper, dodecane (2.0 mL), dibenzyl ether (0.1 mmol), and catalyst (100 mg) were added. The sealed tube was stirred in an oil bath at 140 °C for a setting reaction time. As shown in **Figure S14**, the presence of MoO_2 resulted in a notable increase in toluene content compared to reactions without the catalyst. Moreover, an increase in toluene content was observed with longer reaction times, indicating that toluene was formed through the autolytic decomposition of dibenzyl ether in dodecane.

14. Benzylation of the PX with benzyl alcohol on MoO_2

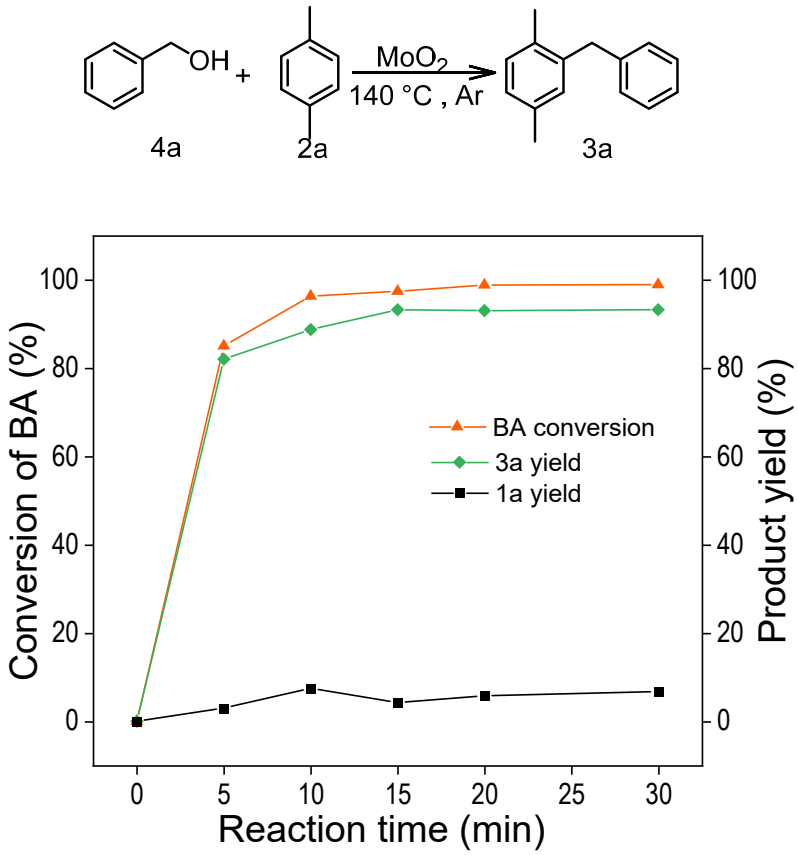

Figure S15. Time profile of benzylation of the PX with benzyl alcohol on MoO_2. Reaction conditions: MoO_2 50 mg, benzyl alcohol 0.1 mmol, PX 2.0 mL, 140 °C, Ar 1 atm.

14. Benzylation of PX with benzyl ethers in the presence of TEMPO

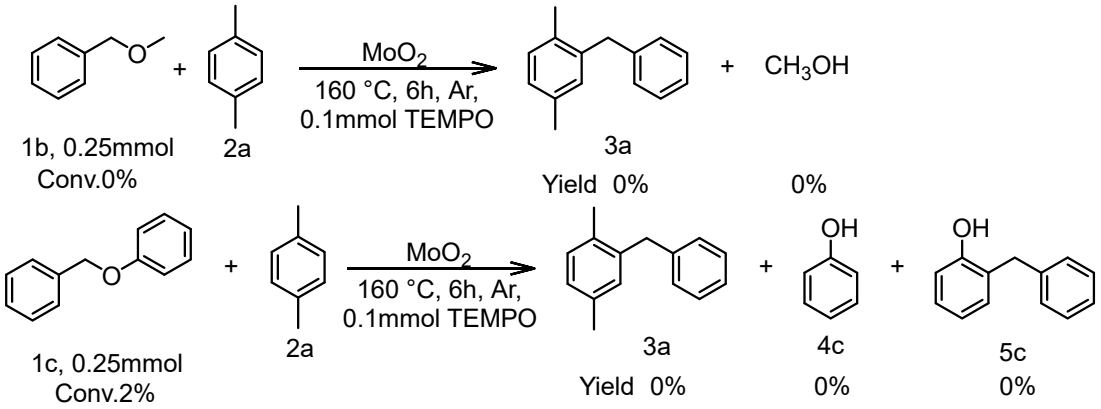

Scheme S3. Benzylation of PX with Benzyl Ethers in the Presence of TEMPO.

The benzylation of PX with of benzyl methyl ether (**1b**) and benzyl phenyl ether (**1c**) could significantly be restrained by TEMPO, which was consistent with the reaction using DBE as substrate. The result indicates that radicals still play a crucial role in the benzylation process with these benzyl ethers as the benzylation reagents.

16. PPh_3 trapping experiment

Table S2: PPh_3 trapping experiment

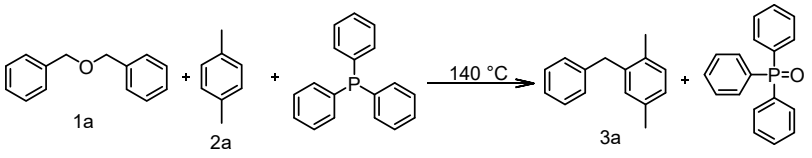

Entry	Substrate	Catalyst	Conv. Of 1a	Yield of 3a	Conv. Of PPh_3	Yield of PPh_3=O
1	DBE	MoO_2	6.3	6.3	78.5	46.6
2	DBE	-	-	-	0.2	0.2
3	-	MoO_2	-	-	78.2	46.3

Reaction conditions: DBE 0.1 mmol, PX 2 mL, catalyst 50 mg, 0.2 mmol of PPh_3, 140 °C, 10 min, Ar atmosphere.

17. DFT calculations

We have employed the Vienna Ab Initio Simulation Package (VASP)[1, 2] to perform all the density functional theory (DFT) calculations within the generalized gradient approximation (GGA) using the PBE[3] formulation. We have chosen the projected augmented wave (PAW) potentials[4, 5] to describe the ionic cores and take valence electrons into account using a plane wave basis set with a kinetic energy cutoff of 450 eV. Partial occupancies of the Kohn−Sham orbitals were allowed using the Gaussian smearing method and a width of 0.05 eV. The on-site corrections (DFT+U) have been applied to the 4d electron of Mo atoms (U_{eff}=4.4 eV) by the approach from Dudarev.[6] The electronic energy was considered self-consistent when the energy change was smaller than 10^{-5} eV. A geometry optimization was considered convergent when the force change was smaller than 0.02 eV/Å. Grimme's DFT-D3 methodology[7] was used to describe the dispersion interactions. The equilibrium lattice constants of the monoclinic MoO_2 unit cell were optimized to be a=5.633 Å, b=4.912 Å, c=5.508 Å, α=90°,β=120.1°, and γ=90°. We then use it to construct a MoO_2(011) surface model with *p*(2×2) periodicity in the X and Y directions and two stoichiometric layers in the Z direction by vacuum depth of 15 Å in order to separate the surface slab from its periodic duplicates. This model comprises 32 Mo and 64 O atoms. During structural optimizations, a 2×2×1 k-point grid in the Brillouin zone was used for k-point sampling, and the bottom stoichiometric layer was fixed while the rest were allowed to fully relax.

The adsorption energy (E_{ads}) of adsorbate A was defined as

$$E_{ads} = E_{A/surf} - E_{surf} - E_{A(g)}$$

where $E_{A/surf}$, E_{surf} and $E_{A(g)}$ are the energy of adsorbate A adsorbed on the surface, the energy of clean surface, and the energy of isolated A molecule in a cubic periodic box with a side length of 20 Å, respectively.

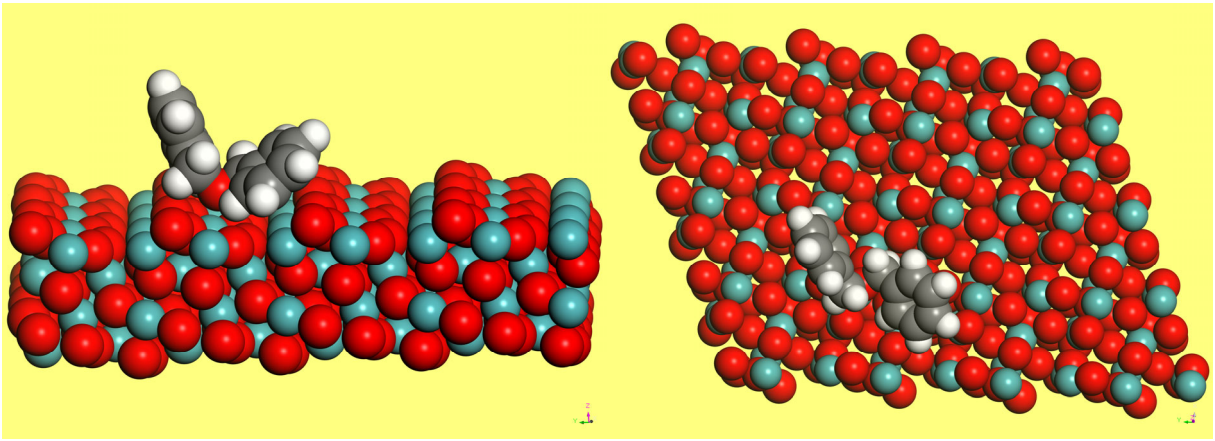

A* (Side View, BnOBn*)　　A* (Top View, BnOBn*)

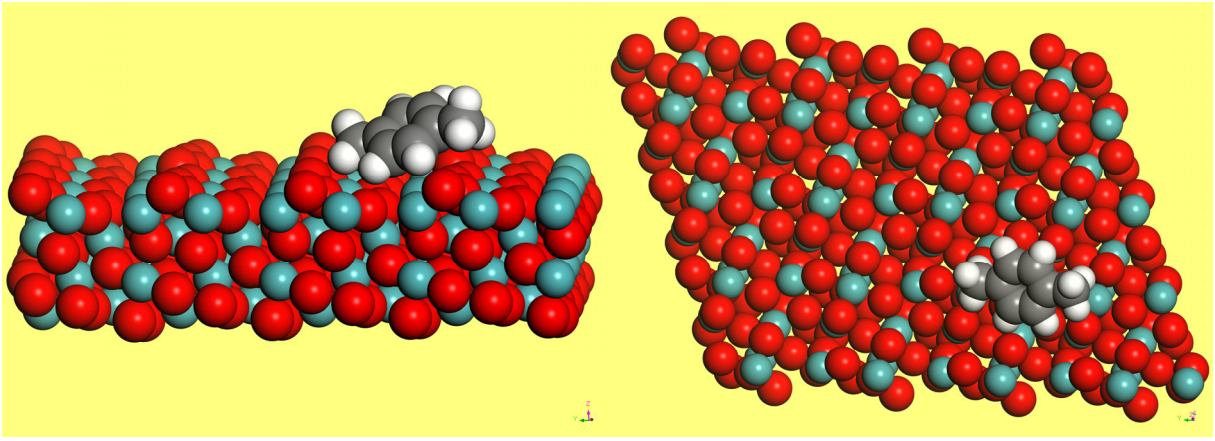

B* (Side View, PX*)　　B* (Top View, PX*)

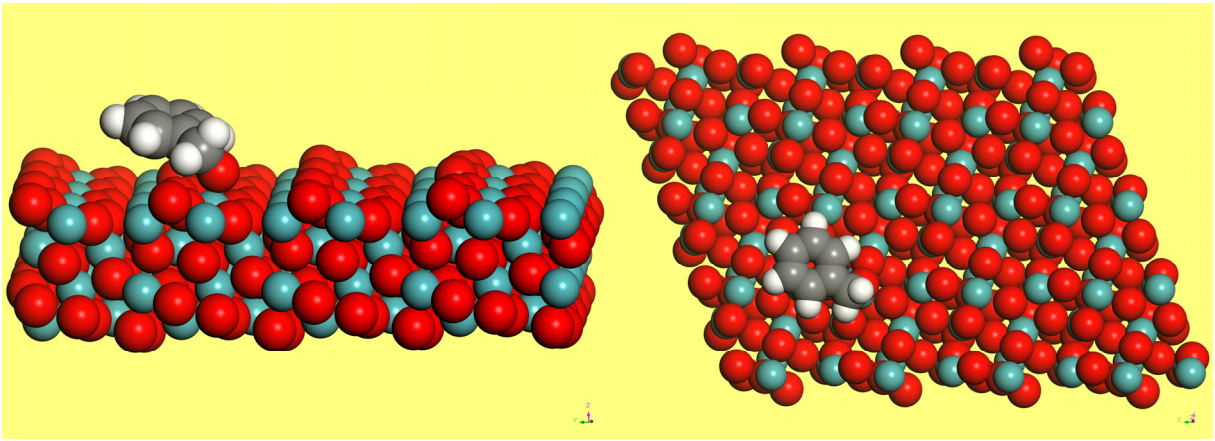

C* (Side View, BnO•*)　　C* (Top View, BnO•*)

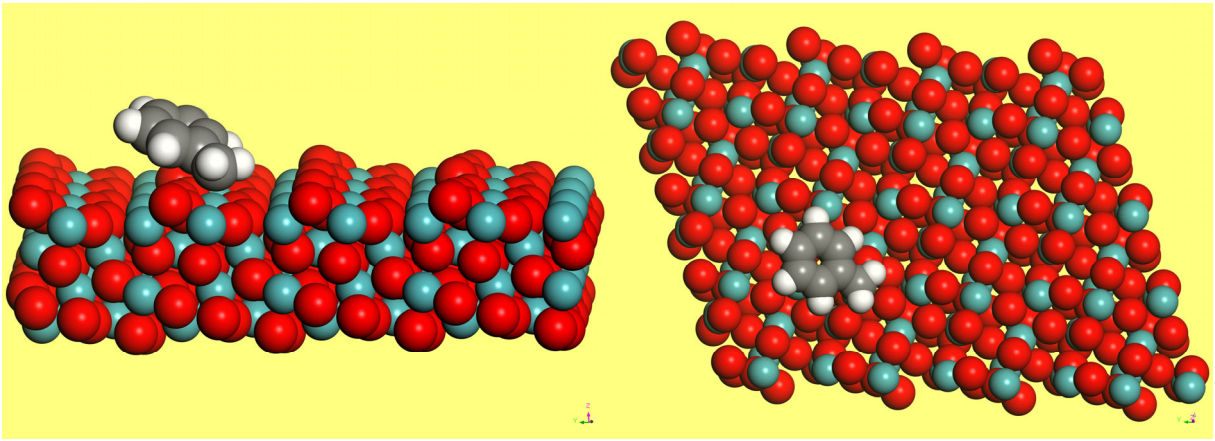

D* (Side View, Bn•*) **D* (Top View, Bn•*)**

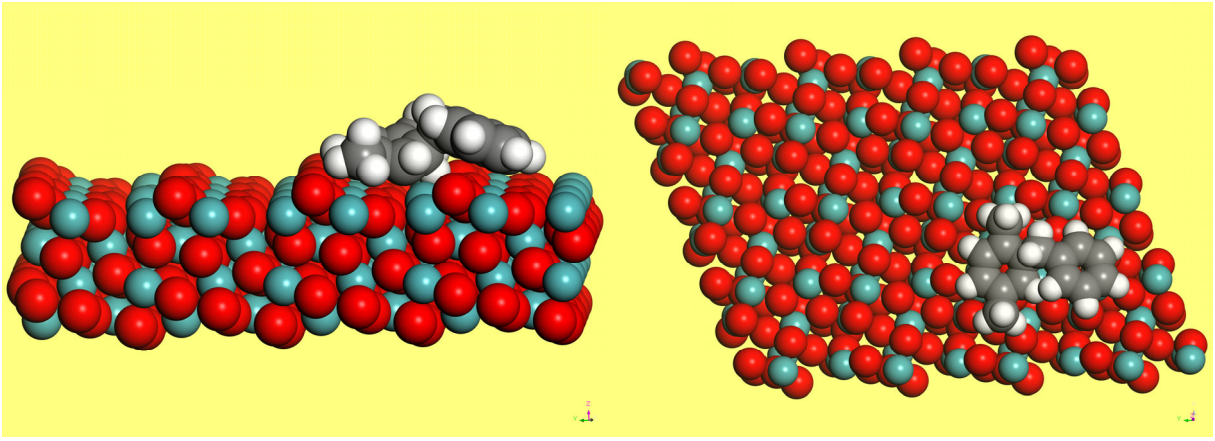

E* (Side View) **E* (Top View)**

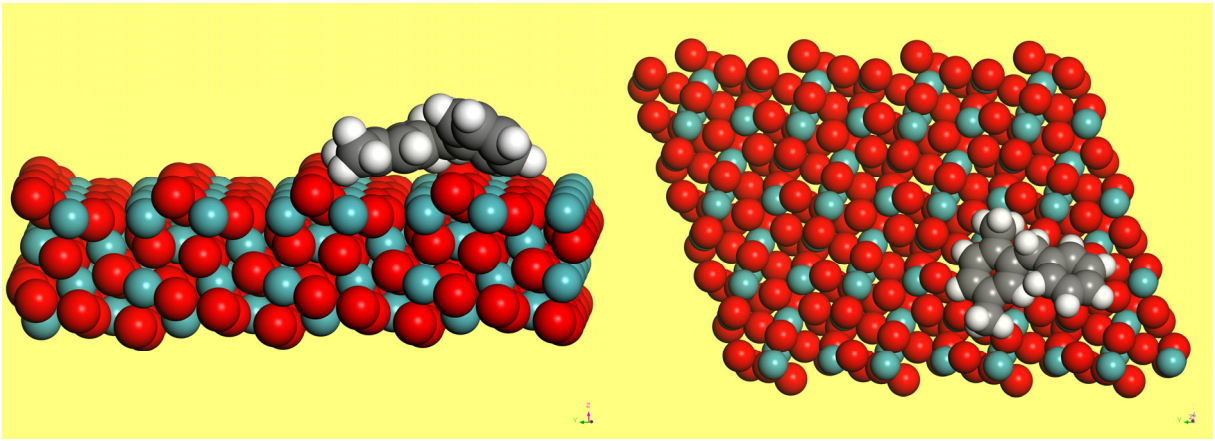

F* (Side View) **F* (Top View)**

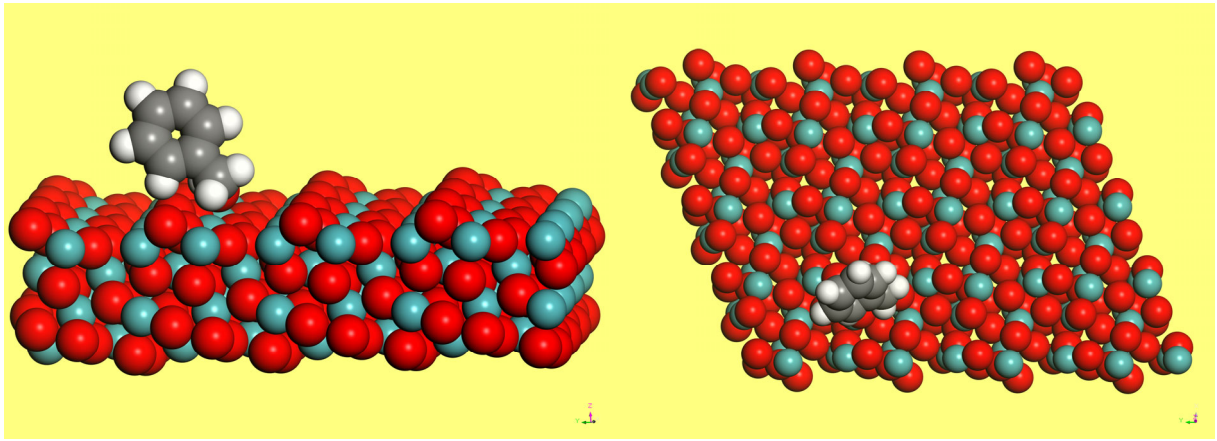

G* (Side View, BnOH*) **G* (Top View, BnOH*)**

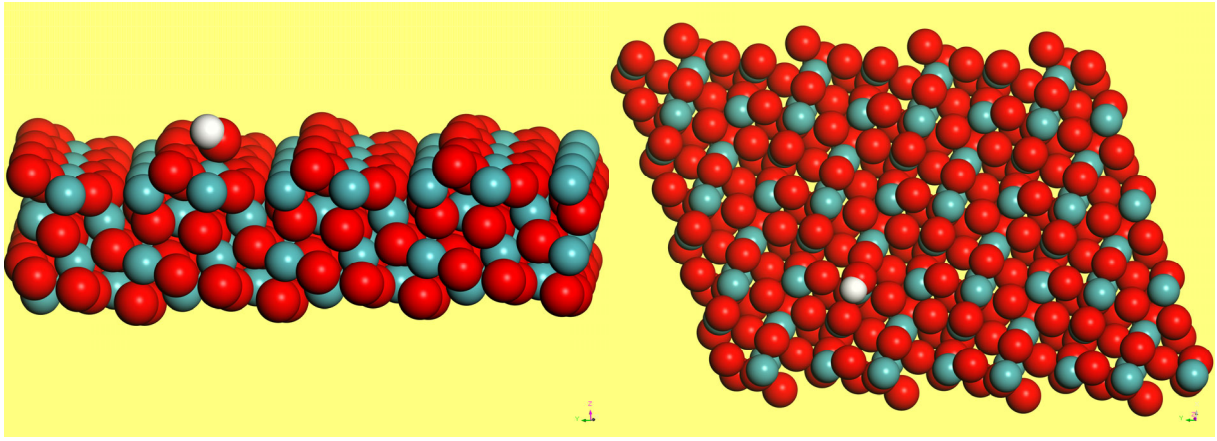

H* (Side View, HO*) **H* (Top View, HO*)**

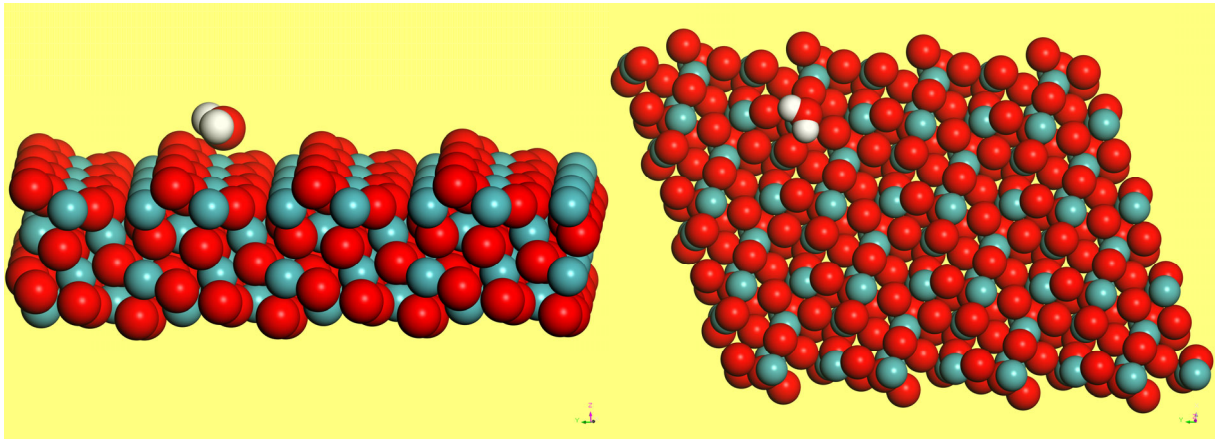

I* (Side View, H_2O *) **I* (Top View, H_2O *)**

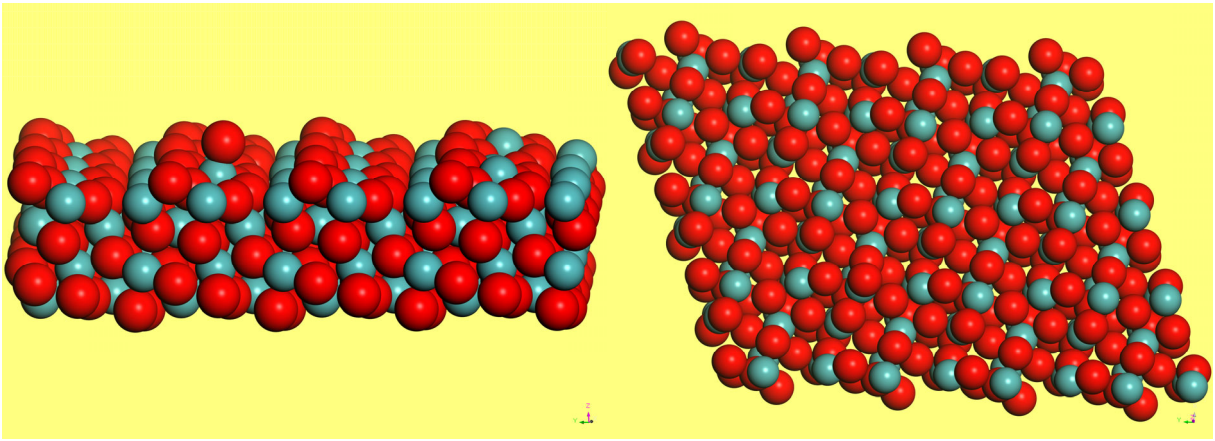

J* (Side View, O*) **J * (Top View, O*)**

Figure S16. The molecular adsorption states of various intermediates

18. Substrate Expansion

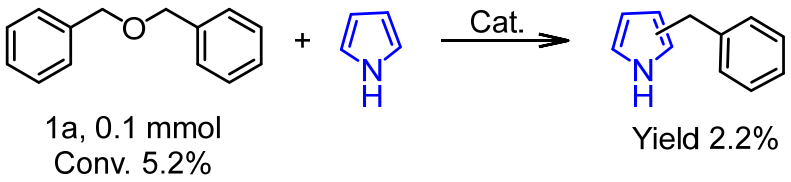

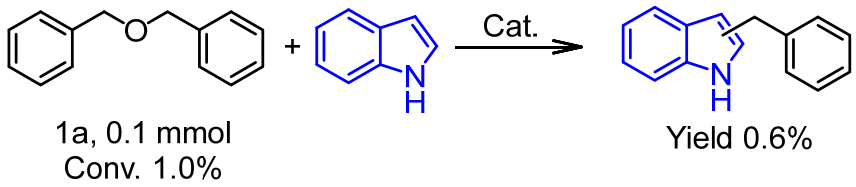

Scheme S4. Benzylation of N-heterocyclic compounds.

We also examined the effects of benzylation on electron-rich N-containing heterocyclic compounds, such as pyrrole and indole, under the following reaction conditions: DBE (0.1 mmol), MoO_2 (50 mg), and arene solvent (2 mL) were heated to 140 °C in a 15 mL pressure-resistant flask on an oil bath with stirring for a certain time. The above electron-rich N-containing heterocyclic compounds exhibit poor activity as shown in **Scheme S4.**

19. Gram-scale reaction experiment

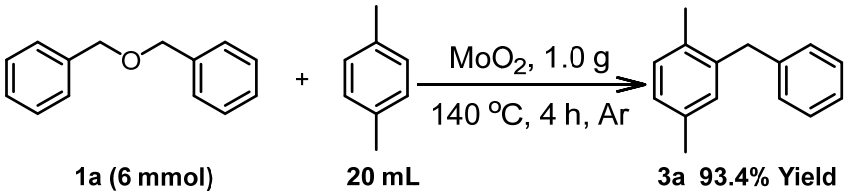

The optimal reaction conditions for this system were applied to the scale-up reaction. DBE (6 mmol), MoO_2 (1.0 g), and PX (20 mL) were heated to 140 °C in a 150 mL pressure-resistant flask on an oil bath with stirring for a certain time. After the reaction was completed, the reaction solution was cooled to room temperature and filtered to remove the catalyst. The organic phase was analyzed by GC/MS using n-dodecane as an internal standard. The substrate **1a** was completely converted within 4 h, providing a 93.4% yield of 2-benzyl-1,4-dimethylbenzene (**3a**).

20. Comparison of recently studied benzylation reaction systems

Table S3. Recent advances in the benzylation reaction systems

Entry	Substrate	Benzylation Reagent	Catalyst	Solvent	Conditions	Conv./Yield (benzylation)	Ref.
1	Anisole	Benzyl alcohol	H_2[MIMPS]$PW_{12}O_{40}$	---	155 °C，2 h	99%/98%	[8]
2	p-xylene	Benzyl alcohol	[SO_3H-PMIm][OTf]	---	120 °C，12 h	99%/96%	[9]
3	toluene	benzyl alcohol	BF_3-H_2O	toluene	Benzylic alcohol (1.0 mmol), toluene (2.0 mL), BF_3-OEt_2 2 equiv., 80 °C, 2 h.	---/96%	[10]
4	p-xylene	Benzyl fluoride	HF	HFIP/DCE (1:9)	r.t. , 18 h	95%/90%	[11]
5	p-xylene	Benzyl bromide	$InCl_3$	CH_2Cl_2	r.t，16 h	99%/99%	[12]
6	o-xylene	4-chlorostyrene	3$FeCl_3$ 6H_2O/Gly	DES	120 °C，7 h	99%/93%	[13]
7	p-xylene	Benzyl alcohol	$HfCl_4$/HfO_2	---	80 °C，40 h	99%/87%	[14]
8	1,3-dicarbonyl compounds	Benzyl Alcohol	Fe(OTf)$_3$–$N_{4111}NTf_2$	-	80 °C，6 h	99%/92-96%	[15]
9	Benzene	Benzyl bromide	Et_3Si-($HCB_{11}H_5Br_6$)	---	r.t.，1 h	99%/95%	[16]
10	benzene	dibenzyl ether	$AgClO_4$–$SnCl_4$	benzene	Room temperature, 3.5 h.	/83%	[17]
11	p-xylene	benzyl methyl ether	$FeCl_3$	p-xylene	Arene (1 mL), benzyl methyl ether (0.5 mmol), $FeCl_3$ (10.0 mol%), 90 °C, 12h.	---/90%	[18]
12	benzene	benzyl alcohol	Sm(OTf)$_3$	benzene	Benzyl reagent 1.0 mmol, benzene 5.0 mL, Sm(OTf)$_3$ 0.1 mmol, 115-120 °C, 6 h.	---/94%	[19]
		dibenzyl ether				---/39%	[19]
13	toluene	benzyl silyl ethers	Hf(OTf)$_4$	toluene	10 mol% catalyst, 50 °C, 4.5 h.	---/80%	[20]
14	p-xylene	1-phenylethyl acetate	$H_2[PtCl_6]\cdot 6H_2O$	p-xylene	10 mL o-xylene, 0.5 mmol 1-phenylethyl acetate, 10 mol% catalyst, 80 °C, 20 h.	100%/80%	[21]
15	p-xylene	dibenzyl ether	$[Ir_2(COD)_2(SnCl_3)_2(Cl)_2(\mu\text{-}Cl)_2]$	---	Catalyst 1 mol%, dibenzyl ether 0.25 mmol, PX 8.0 mol, 90 °C, 60 min.	---/82%	[22]
			$[Ir(COD)Cl]_2$ (1%)/$SnCl_4$ (4%)	---	90 °C，1 h	99%/82%	[22]
16	Anisole	Benzyl alcohol	p2NPh-OSO_3H	---	120 °C，4 h	99%/80%	[23]
17	p-xylene	Benzyl alcohol	$Hf_{0.5}$[TEAPS]$PW_{12}O_{40}$	---	140 °C，2 h	99%/99%	[24]
18	mesitylene	benzyl alcohol	Zeolite Beta	mesitylene	Catalyst = 0.1 g; mesitylene = 14 mL; benzyl alcohol 0.2 mL; 100 °C, 30 min.	92%/73%	[25]

19	p-xylene	benzyl alcohol	Montmorillonite K-10	dioxane	A mixture of arene (10 mmol), benzyl benzoate (10 mmol), and montmorillonite K-10 catalyst (500 mg) in dioxane (20 mL), refluxed for 3.0 h.	---/76%	[26]
20	benzene	dibenzyl ether	S–Zr/MCM-41	benzene	The ratio dibenzyl ether and benzene (1:20), catalyst 10 wt%,150 °C, 15 h.	>99%/100%	[27]
21	p-xylene	Benzyl alcohol	Polymer/12-tungstophosphoric acid	p-xylene	Benzyl alcohol (0.05 mol), treated with aromatic substrate (0.3 mol) with PANI supported TPA (0.16 g) at 80 °C for 4 h.	98%/98%	[28]
22	Benzene	Benzyl chloride	FeO_x/HZSM-5	-	80 °C，4 h	92%/88%	[29]
23	Anisole	Benzyl alcohol	P(VB-VMS)PW	-	120 °C，4 h	99%/96.7%	[30]
24	Benzene	Benzyl Chloride	SZF-12	-	80 °C，4 h	87%/85%	[31]
25	Anisole	Benzyl Alcohol	H_2SO_4/Meso Nb	-	120 °C，3 h	99%/92%	[32]
26	Anisole	Benzyl alcohol	Sn_1TPA	---	120 °C，0.5 h	99%/98%	[33]
27	p-xylene	benzyl alcohol	MoO_x	p-xylene	Benzyl alcohol 0.24 mL, arene 15.0 mL, catalyst 0.3 g, Ar,135 °C, 10 min.	99%/99%	[34]
			Heterogeneous	Note: Acid-catalyzed benzyl cation-mediated Friedel–Crafts benzylation mechanism.			
28	Dibenzoyl methane	Tolene	$Fe(OAc)_2$	-	120 °C，24 h	85%/72%	[35]
				Note: Radical coupling mechanism.			
29	N-methylquinoxalin-2(1 *H*)-one	Benzyl bromide	Nucleophilic dithiocarbonate anions	DCE	460 nm LED at 60 °C for 12 h.	99%/90%	[36]
				Note: Photocatalysis, Radical coupling mechanism.			
30	N-Heteroarenes	Benzaldehydes	Rhodamine 6G	MeCN	390 nm LED at 50 °C for 48 h	89%/86%	[37]
				Note: Photocatalysis, Radical coupling mechanism.			
31	p-xylene	dibenzyl ether	2H-MoS_2	p-xylene	Catalyst 100 mg, dibenzyl ether 0.25 mmol, PX 2.0 mL, 140 °C, 10 min.	59.6%/57.1%	[38]
			Heterogeneous	Note: Radical-Friedel–Crafts benzylation mechanism.			
32	p-xylene	dibenzyl ether	MoO_2	p-xylene	Catalyst 100 mg, dibenzyl ether 0.25 mmol, PX 2.0 mL, 140 °C, 10 min.	78.9%/77.7% 99%/99% (60 min)	This work
			Heterogeneous	Note: Radical-Friedel–Crafts benzylation mechanism.			

21. NMR Spectra of some products

2-Benzyl-1,4-dimethylbenzene (3a)

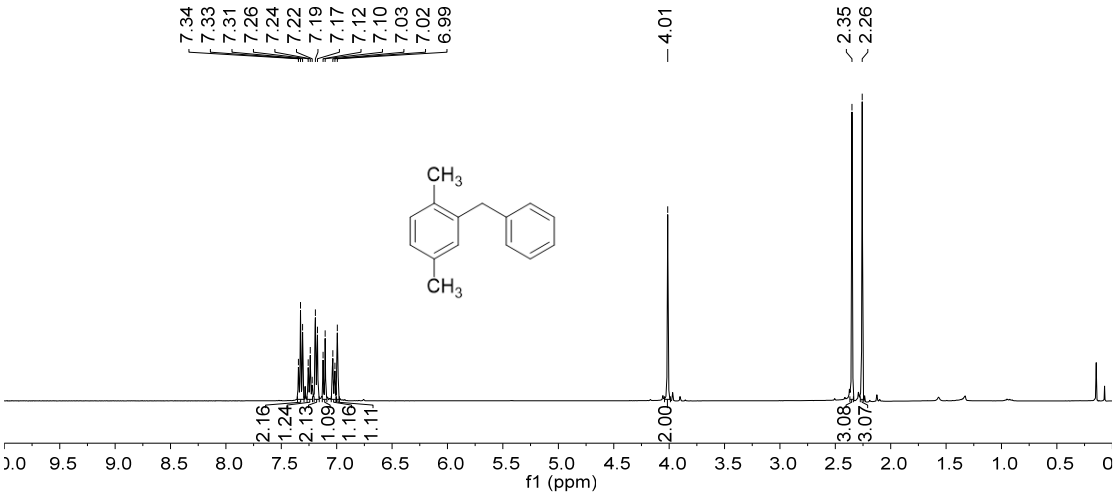

^{1}H NMR (400 MHz, $CDCl_3$) δ 7.33 (t, *J* = 7.2 Hz, 2H), 7.24 (t, *J* = 7.3 Hz, 1H), 7.18 (d, *J* = 7.3 Hz, 2H), 7.11 (d, *J* = 7.6 Hz, 1H), 7.03 (d, *J* = 7.7 Hz, 1H), 6.99 (s, 1H), 4.01 (s, 2H), 2.35 (s, 3H), 2.26 (s, 3H).

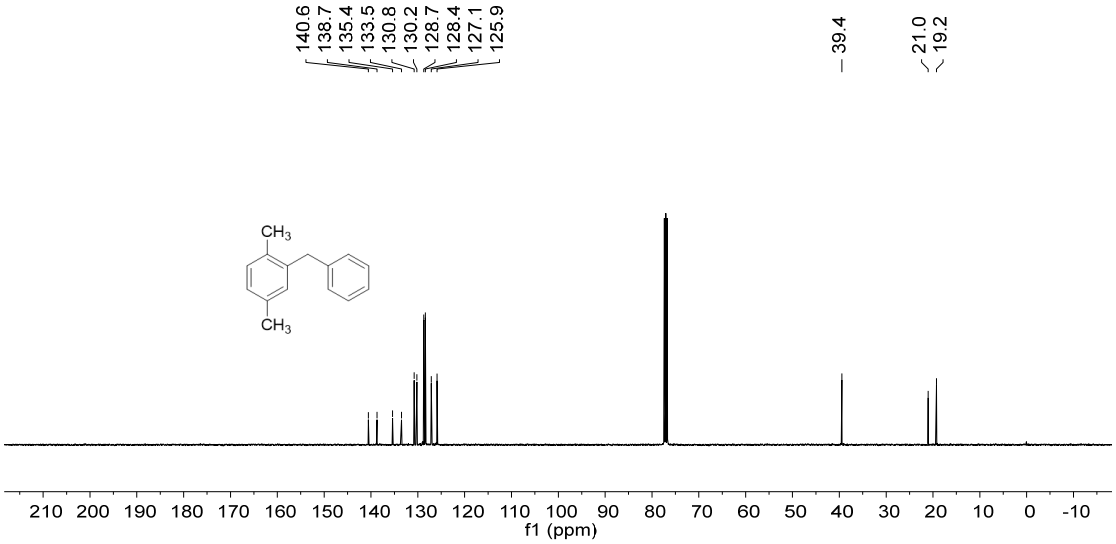

^{13}C NMR (100 MHz, $CDCl_3$) δ 140.6, 138.7, 135.4, 133.5, 130.8, 130.2, 128.7, 128.4, 127.1, 125.9, 39.4, 21.0, 19.2.

Diphenylmethane (Table 2, entry 1)

^{1}H NMR (400 MHz, $CDCl_3$) δ 7.40 – 7.32 (m, 4H), 7.31 – 7.23 (m, 6H), 4.06 (s, 2H).

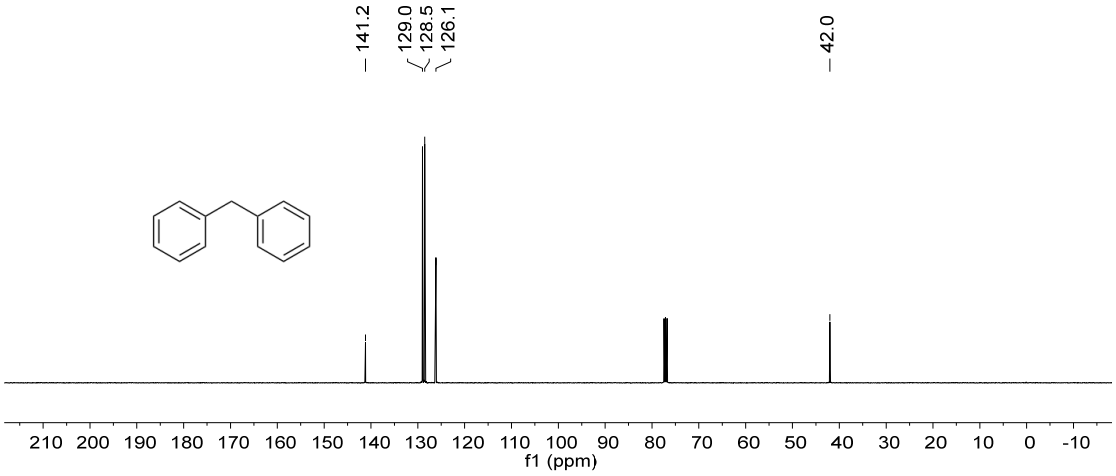

^{13}C NMR (100 MHz, $CDCl_3$) δ 141.2, 129.0, 128.5, 126.1, 42.0.

4-Methyldiphenylmethane (Table 2, entry 2)

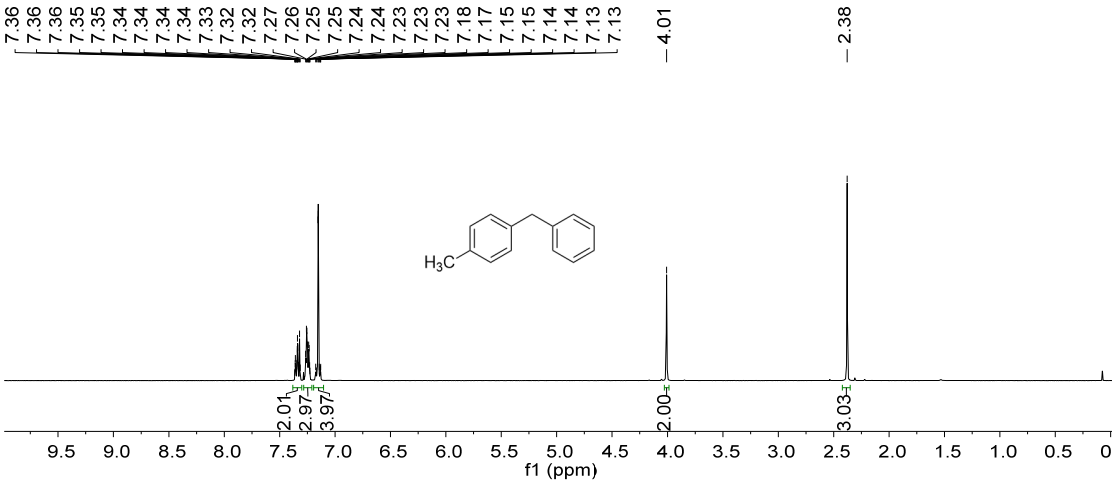

^{1}H NMR (400 MHz, $CDCl_3$) δ 7.38 – 7.30 (m, 2H), 7.28 – 7.21 (m, 3H), 7.19 – 7.10 (m, 4H), 4.01 (s, 2H), 2.38 (s, 3H).

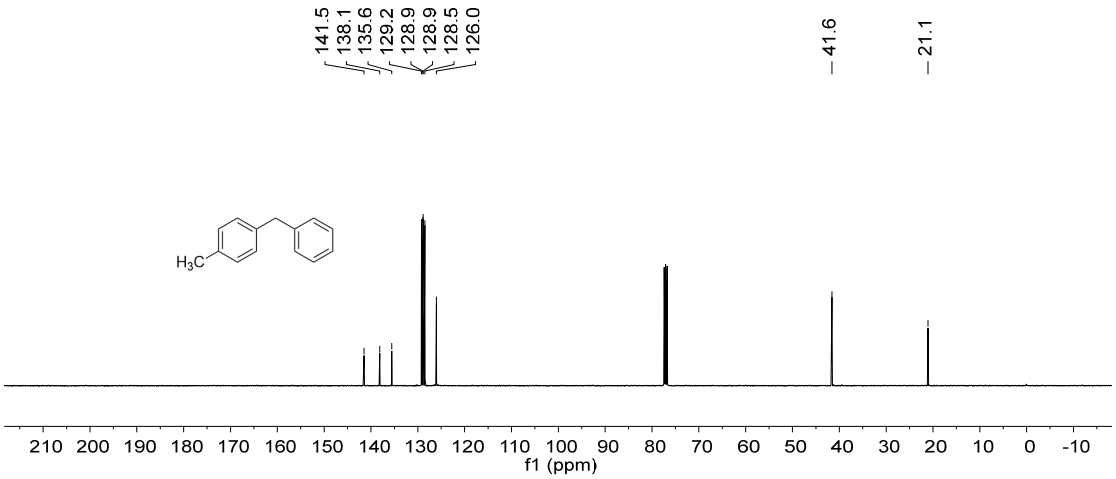

^{13}C NMR (100 MHz, $CDCl_3$) δ 141.5, 138.1, 135.6, 129.2, 128.92, 128.86, 128.5, 126.0, 41.6, 21.1.

4-Methoxydiphenylmethane (Table 2, entry 5)

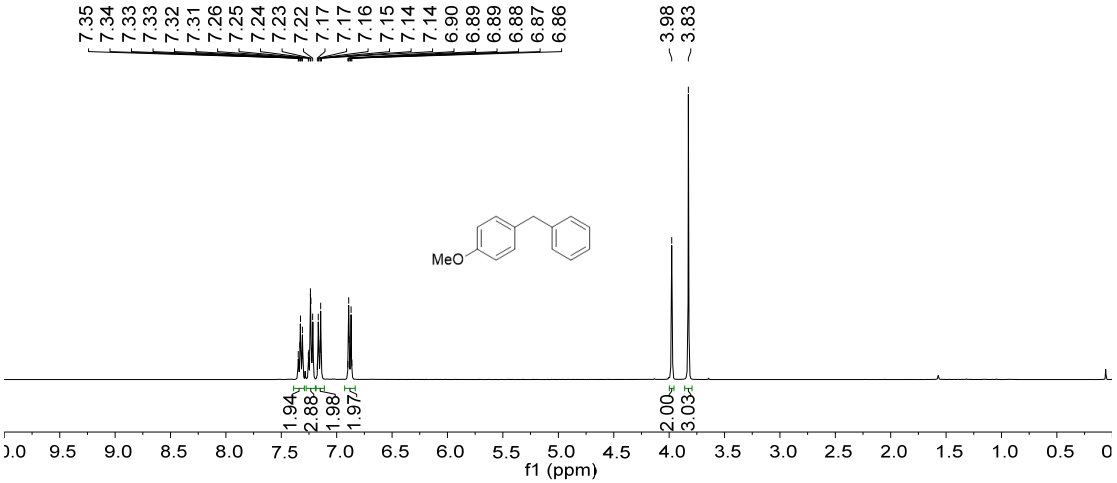

^{1}H NMR (400 MHz, $CDCl_3$) δ 7.39 – 7.29 (m, 2H), 7.28 – 7.19 (m, 3H), 7.19 – 7.11 (m, 2H), 6.93 – 6.83 (m, 2H), 3.98 (s, 2H), 3.83 (s, 3H).

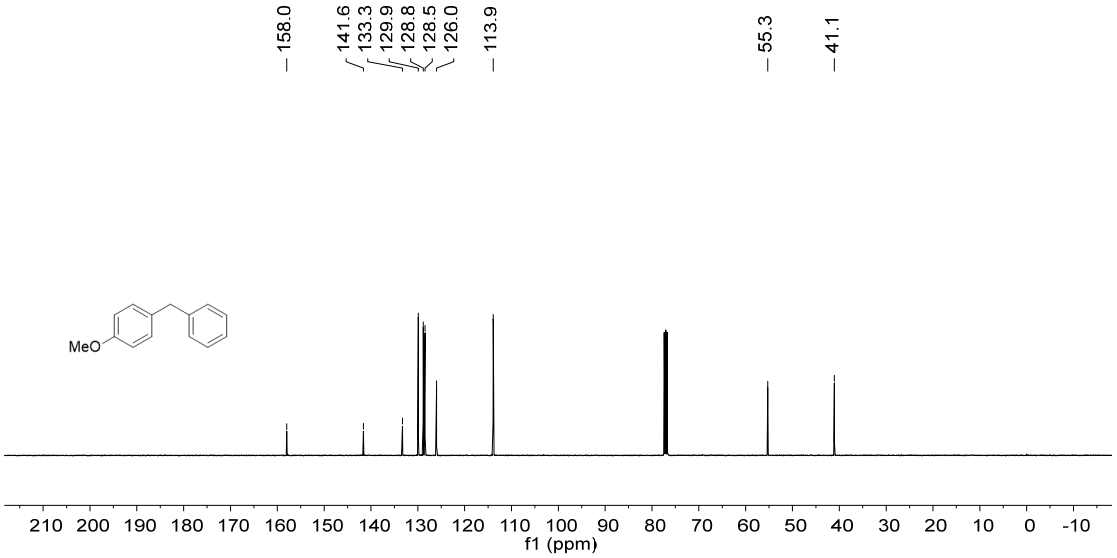

^{13}C NMR (100 MHz, $CDCl_3$) δ 158.0, 141.6, 133.3, 129.9, 128.8, 128.5, 126.0, 113.9, 55.3, 41.1.

2-Benzylnaphthalene (Table 2, entry 7)

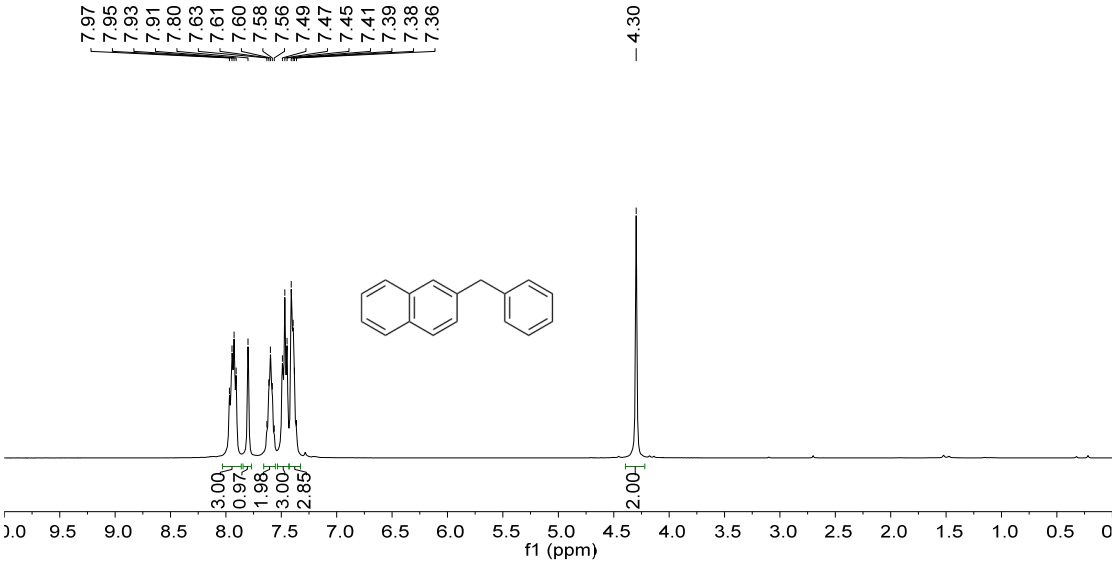

^{1}H NMR (400 MHz, $CDCl_3$) δ 8.03 – 7.86 (m, 3H), 7.80 (s, 1H), 7.66 – 7.55 (m, 2H), 7.53 – 7.43 (m, 3H), 7.43 – 7.32 (m, 3H), 4.30 (s, 2H).

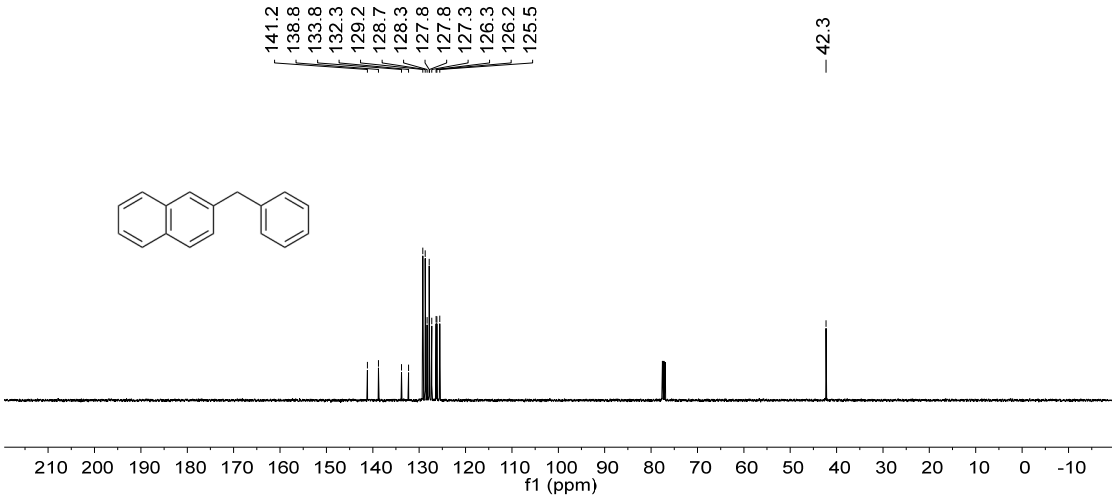

^{13}C NMR (100 MHz, $CDCl_3$) δ 141.2, 138.8, 133.8, 132.3, 129.2, 128.7, 128.3, 127.83, 127.76, 127.3, 126.3, 126.2, 125.5, 42.3.

1-(2-benzylphenyl)ethan-1-one (Table 2, entry 8)

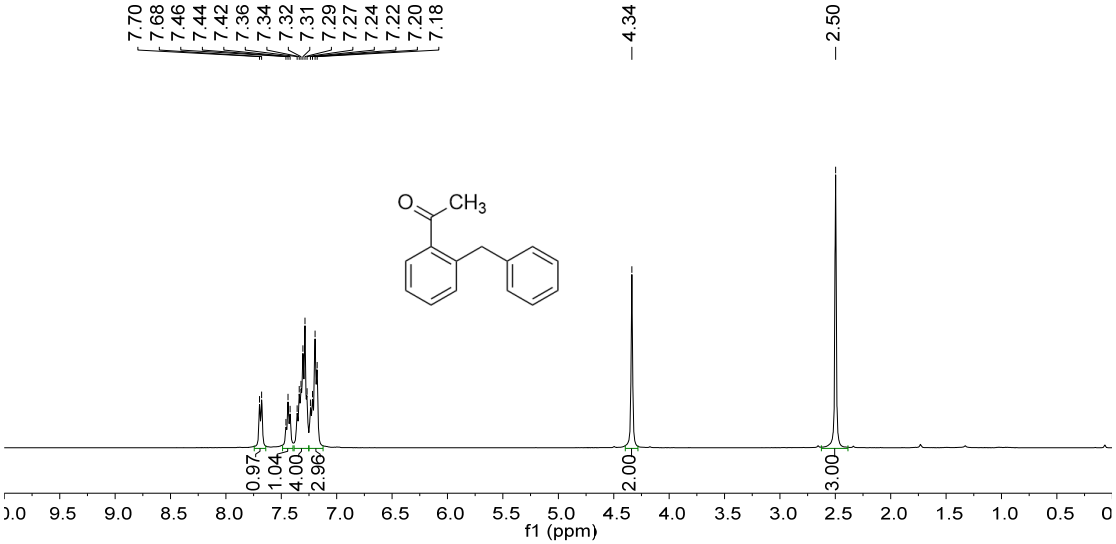

^{1}H NMR (400 MHz, $CDCl_3$) δ 7.69 (d, *J* = 7.7 Hz, 1H), 7.44 (t, *J* = 7.6 Hz, 1H), 7.38 – 7.25 (m, 4H), 7.25 – 7.12 (m, 3H), 4.34 (s, 2H), 2.50 (s, 3H).

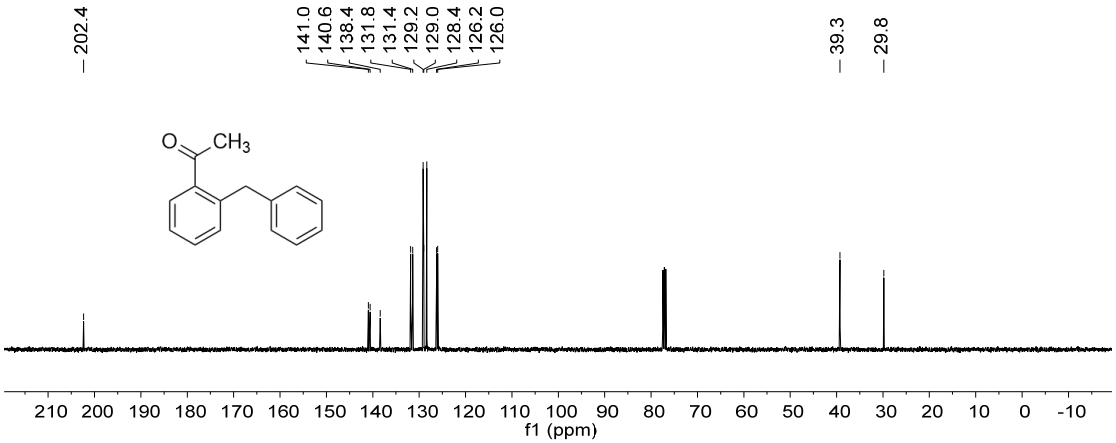

^{13}C NMR (100 MHz, $CDCl_3$) δ 202.4, 141.0, 140.6, 138.4, 131.8, 131.4, 129.2, 129.0, 128.4, 126.2, 126.0, 39.3, 29.8.

4-Chlorodiphenylmethane (Table 2, entry 9)

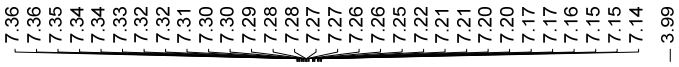

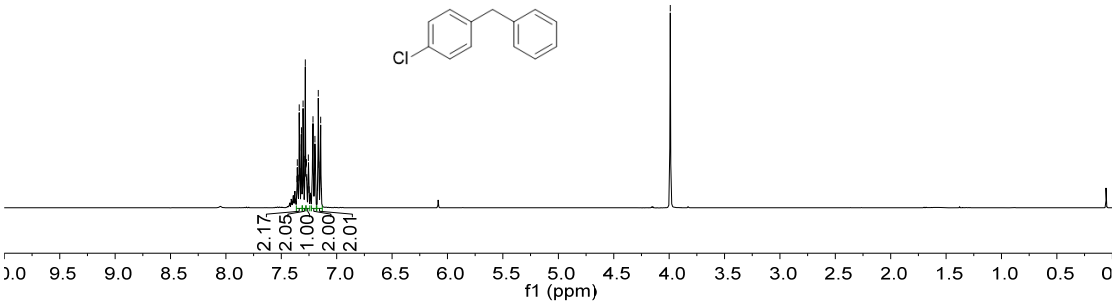

^{1}H NMR (400 MHz, $CDCl_3$) δ 7.36 – 7.31 (m, 2H), 7.31 – 7.28 (m, 2H), 7.28 – 7.24 (m, 1H), 7.23 – 7.18 (m, 2H), 7.18 – 7.13 (m, 2H), 3.99 (s, 2H).

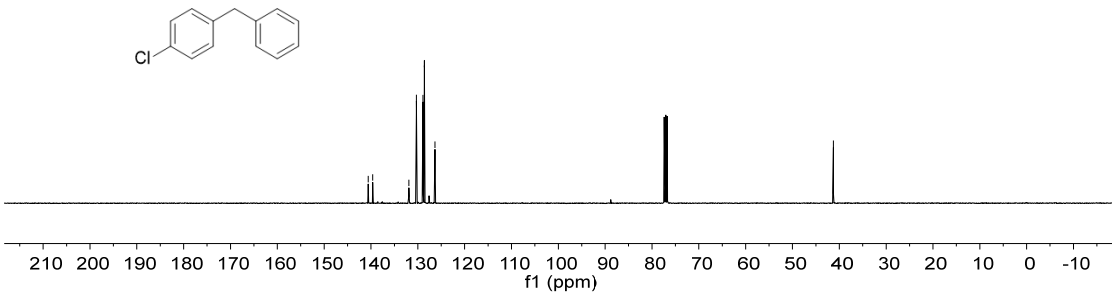

^{13}C NMR (100 MHz, $CDCl_3$) δ 140.6, 139.6, 131.9, 130.3, 128.9, 128.60, 128.60, 126.3, 41.3.

1-Benzyl-4-bromobenzene (Table 2, entry 10)

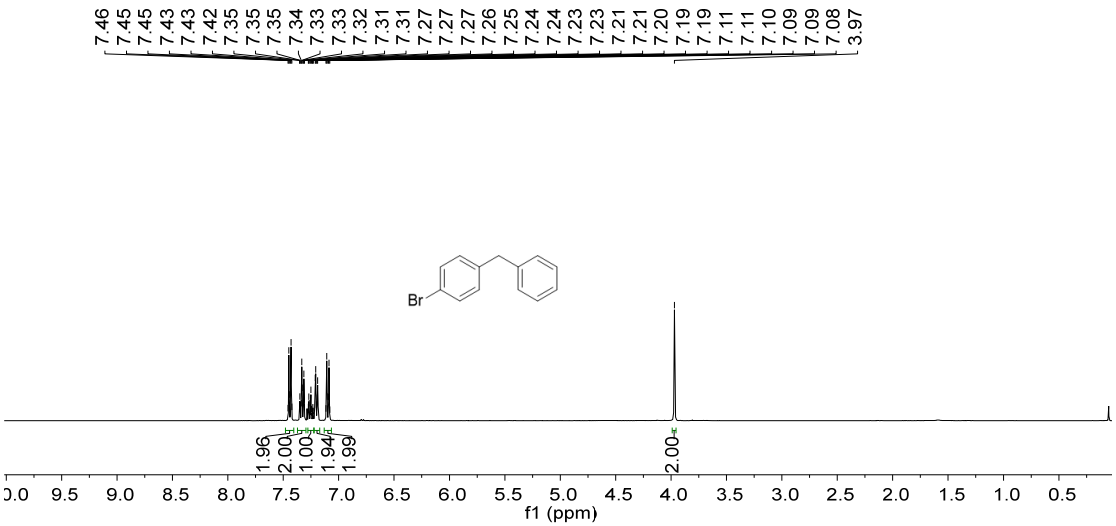

^{1}H NMR (400 MHz, $CDCl_3$) δ 7.48 – 7.41 (m, 2H), 7.37 – 7.29 (m, 2H), 7.28 – 7.22 (m, 1H), 7.22 – 7.17 (m, 2H), 7.13 – 7.06 (m, 2H), 3.97 (s, 2H).

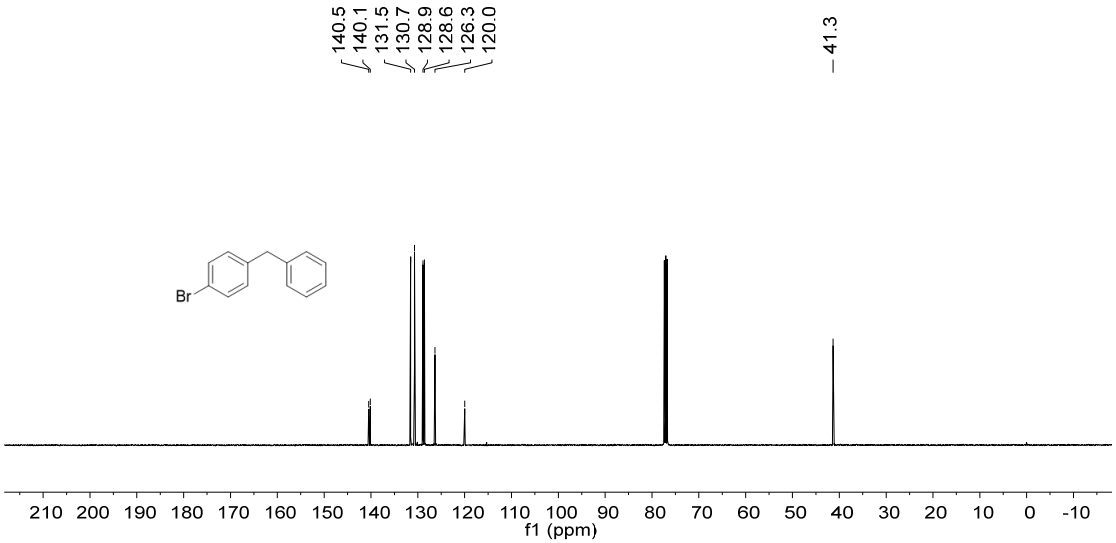

^{13}C NMR (100 MHz, $CDCl_3$) δ 140.5, 140.1, 131.5, 130.7, 128.9, 128.6, 126.3 120.0, 41.3.

3-benzylpyridine (Table 2, entry 11)

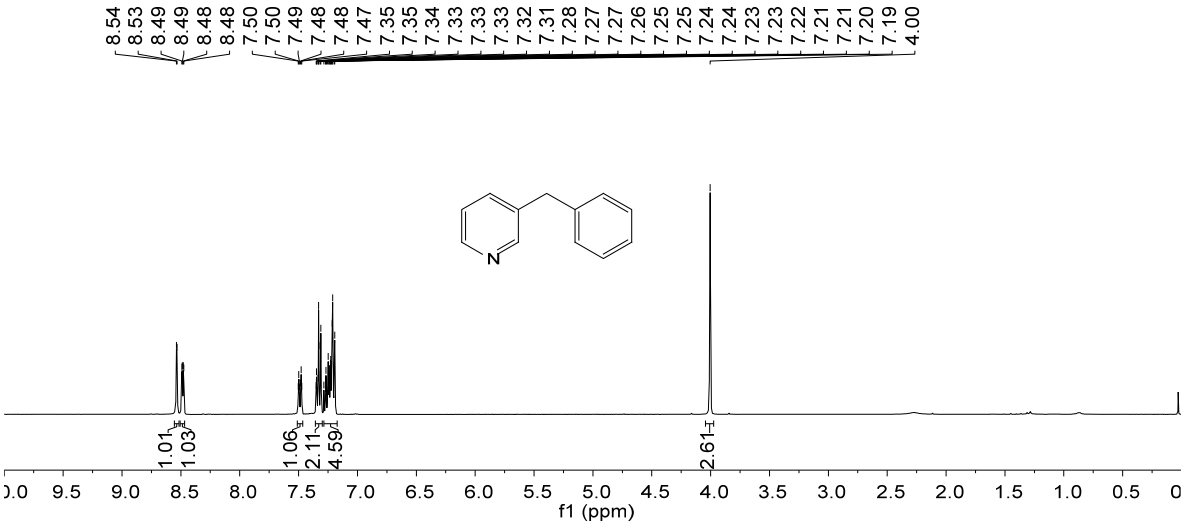

^{1}H NMR (400 MHz, $CDCl_3$) δ 8.53 (d, *J* = 2.3 Hz, 1H), 8.49 (dd, *J* = 4.8, 1.7 Hz, 1H), 7.49 (dt, *J* = 7.9, 2.1 Hz, 1H), 7.36 – 7.30 (m, 2H), 7.28 – 7.17 (m, 4H), 4.00 (s, 2H).

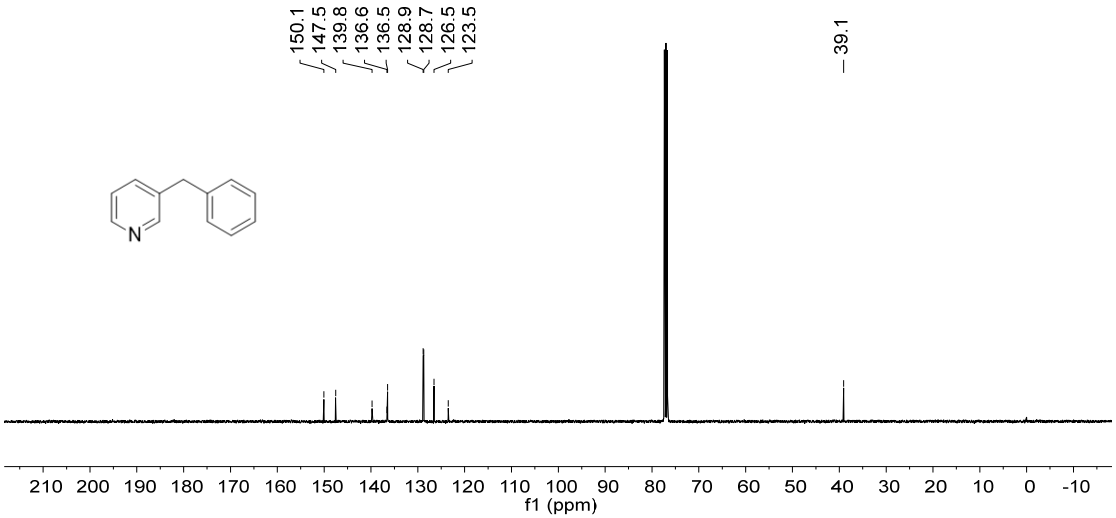

^{13}C NMR (100 MHz, $CDCl_3$) δ 150.1, 147.5, 139.8, 136.6, 136.5, 128.9, 128.7, 126.5, 123.5, 39.1.

5-benzylquinoline (Table 2, entry 12)

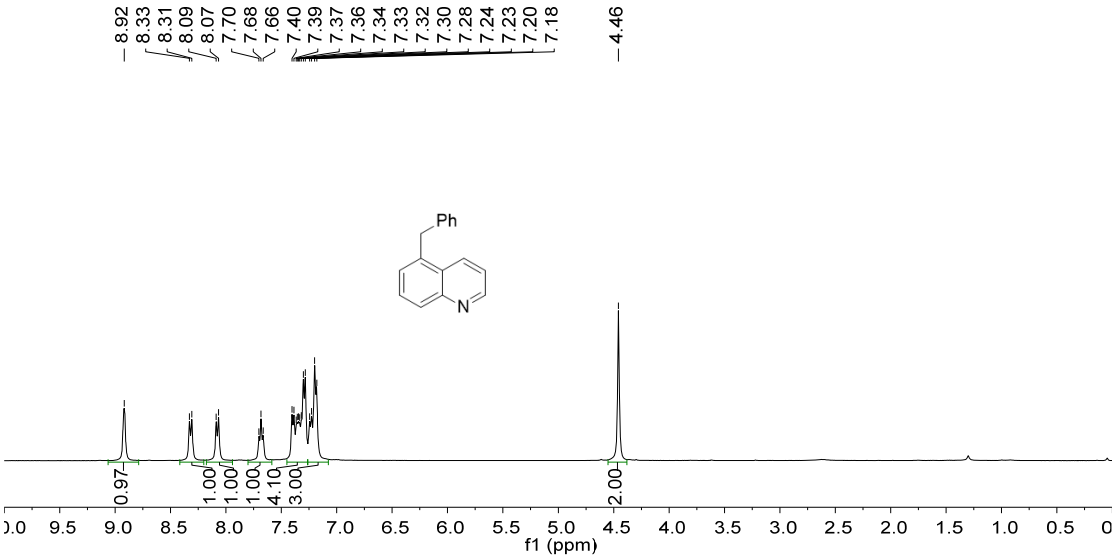

^{1}H NMR (400 MHz, $CDCl_3$) δ 8.92 (s, 1H), 8.49 (d, *J* = 8.5 Hz, 1H), 7.49 (d, *J* = 8.5 Hz, 1H), 7.68 (t, *J* = 7.8 Hz, 1H), 7.45 – 7.26 (m, 4H), 7.26 – 7.07 (m, 3H), 4.46 (s, 2H).

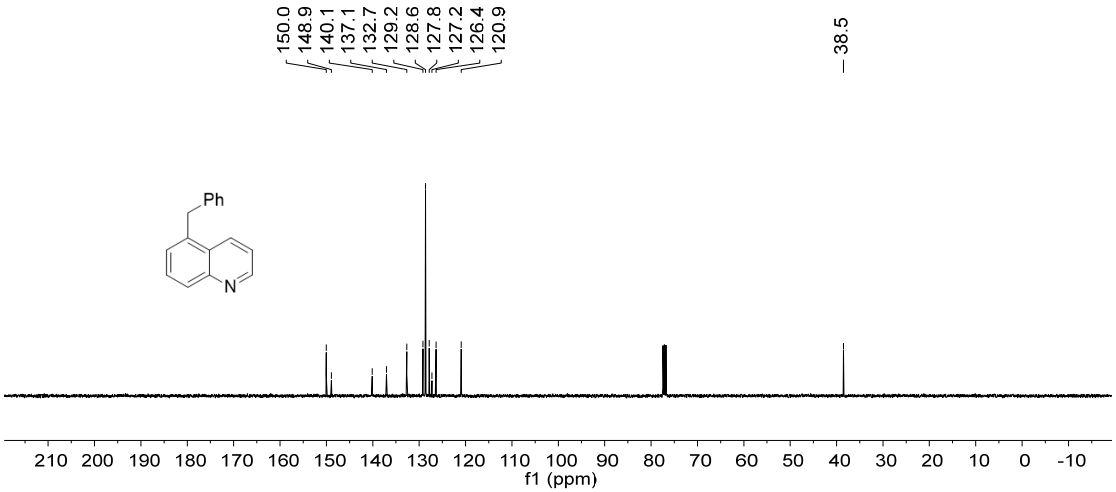

^{13}C NMR (100 MHz, $CDCl_3$) δ 150.0, 148.9, 140.1, 137.1, 132.7, 129.2, 128.6, 127.8, 127.2, 126.4, 120.9, 38.5.

2-(4-chlorobenzyl)-1,4-dimethylbenzene (Table 2, entry 14)

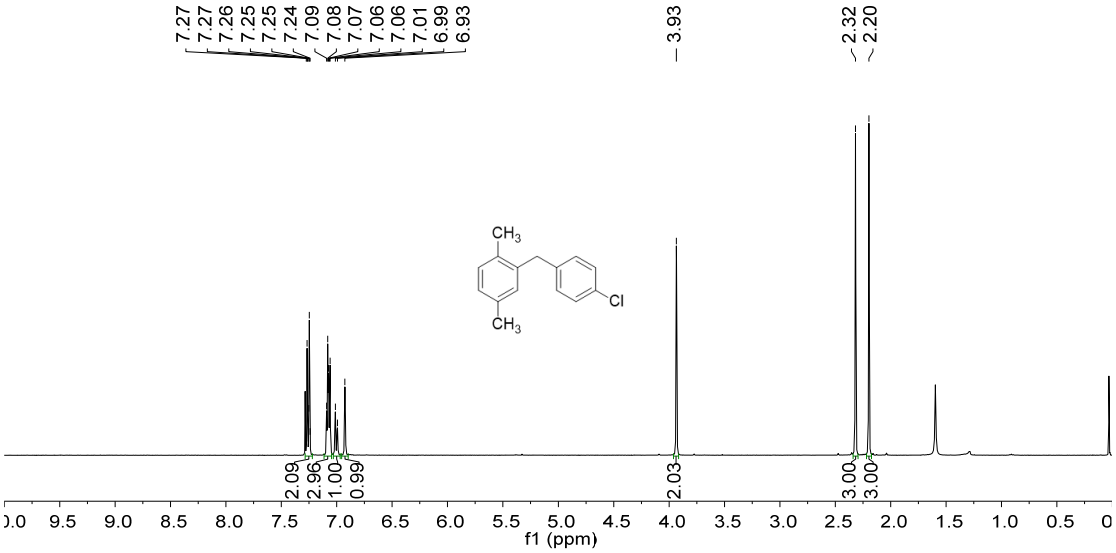

^{1}H NMR (400 MHz, $CDCl_3$) δ 7.28 – 7.22 (m, 2H), 7.11 – 7.05 (m, 3H), 7.00 (d, *J* = 7.7 Hz), 6.93 (s, 1H), 3.93 (s, 2H), 2.32 (s, 3H), 2.20 (s, 3H).

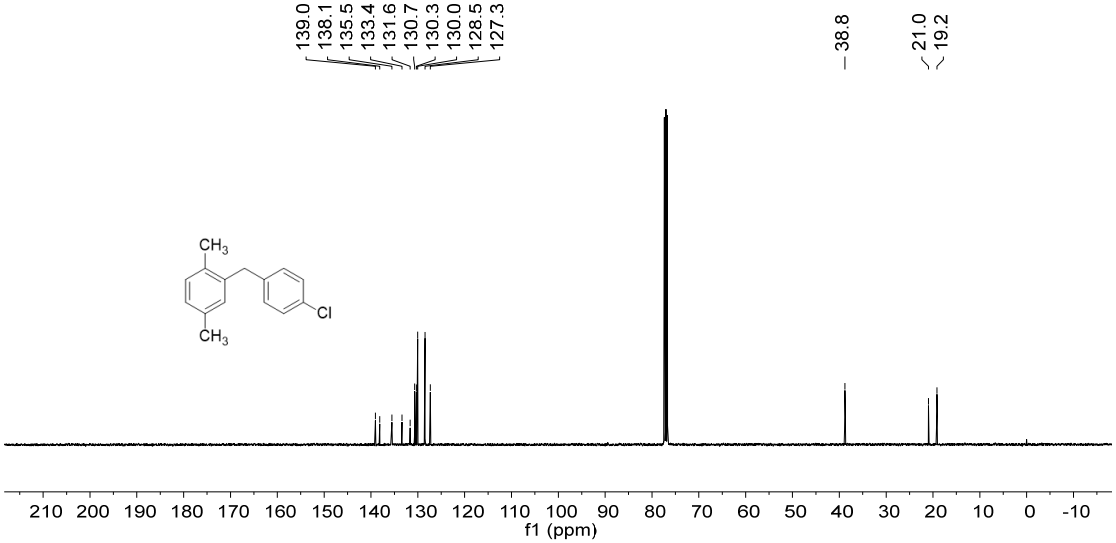

^{13}C NMR (100 MHz, $CDCl_3$) δ 139.0, 138.1, 135.5, 133.4, 131.6, 130.7, 130.3, 130.0, 128.5, 127.3, 38.8, 21.0, 19.2.

2-(4-bromobenzyl)-1,4-dimethylbenzene (Table 2, entry15)

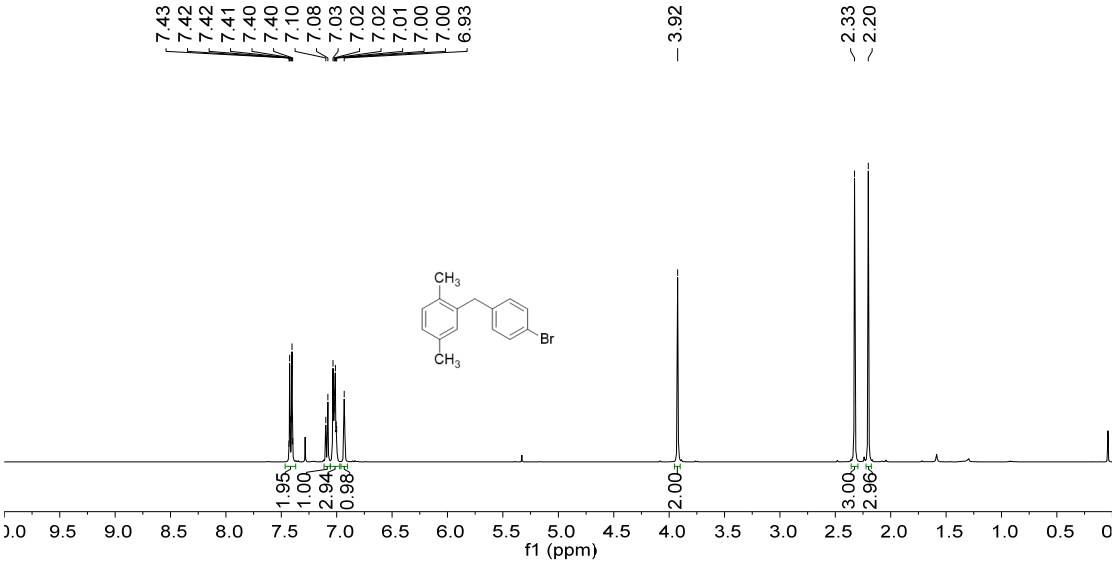

^{1}H NMR (400 MHz, $CDCl_3$) δ 7.46 – 7.37 (m, 2H), 7.09 (d, *J* = 7.6 Hz, 1H), 7.06 – 6.97 (m, 3H), 6.93 (s, 1H), 3.92 (s, 2H), 2.33 (s, 3H), 2.20 (s, 3H).

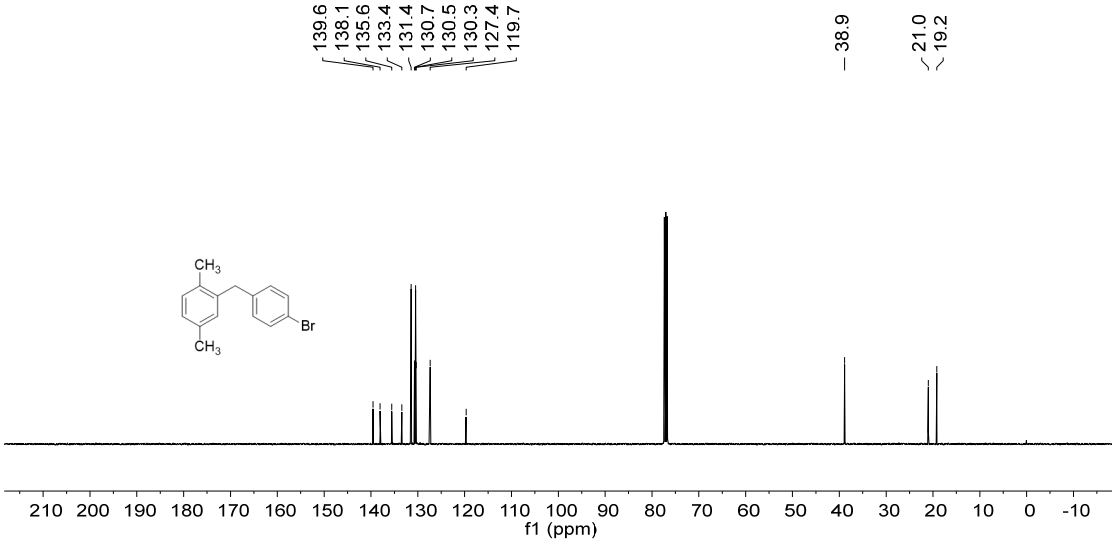

^{13}C NMR (100 MHz, $CDCl_3$) δ 139.6, 138.1, 135.6, 133.4, 131.4, 130.7, 130.5, 130.3, 127.4, 119.7, 38.9, 21.0, 19.2.

1,4-dimethyl-2-(4-methylbenzyl)benzene (Table 2, entry16)

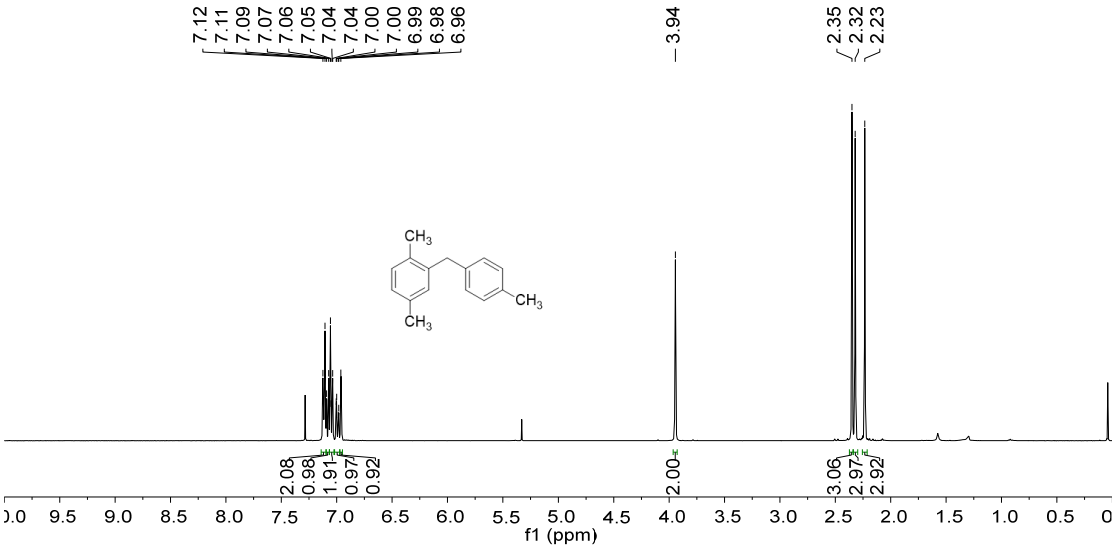

^{1}H NMR (400 MHz, $CDCl_3$) δ 7.12 (d, *J* = 7.9 Hz, 2H), 7.08 (d, *J* = 7.6 Hz, 1H), 7.06 – 7.03 (m, 2H), 7.02 – 6.97 (m, 1H), 6.96 (s, 1H), 3.94 (s, 2H), 2.35 (s, 3H), 2.32 (s, 3H), 2.23 (s, 3H).

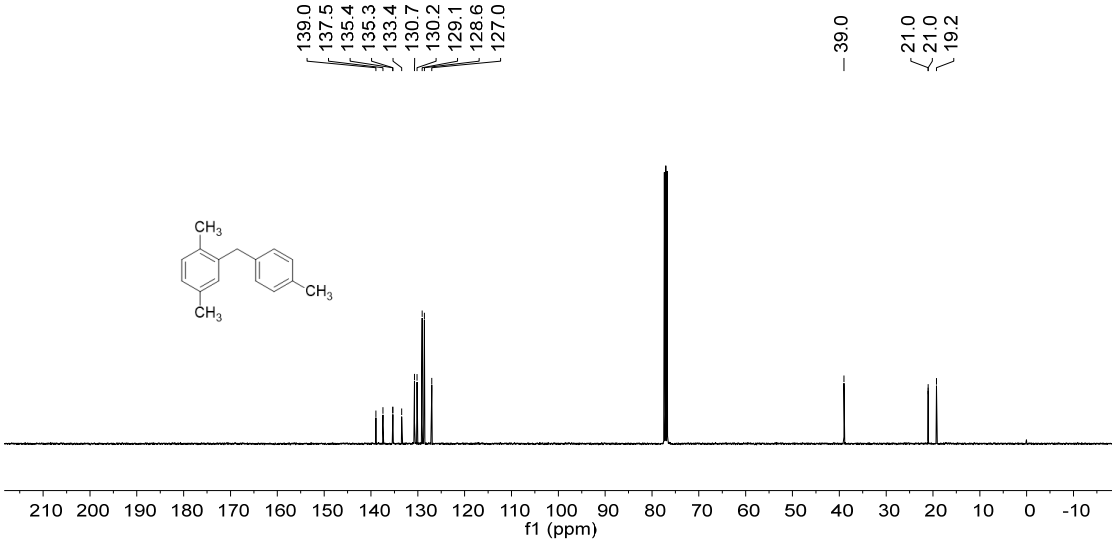

^{13}C NMR (100 MHz, $CDCl_3$) δ 139.0, 137.5, 135.4, 135.3, 133.4, 130.7, 130.2, 129.1, 128.6, 127.0, 39.0, 21.04, 21.02, 19.2.

2-(4-methoxybenzyl)-1,4-dimethylbenzene (Table 2, entry17)

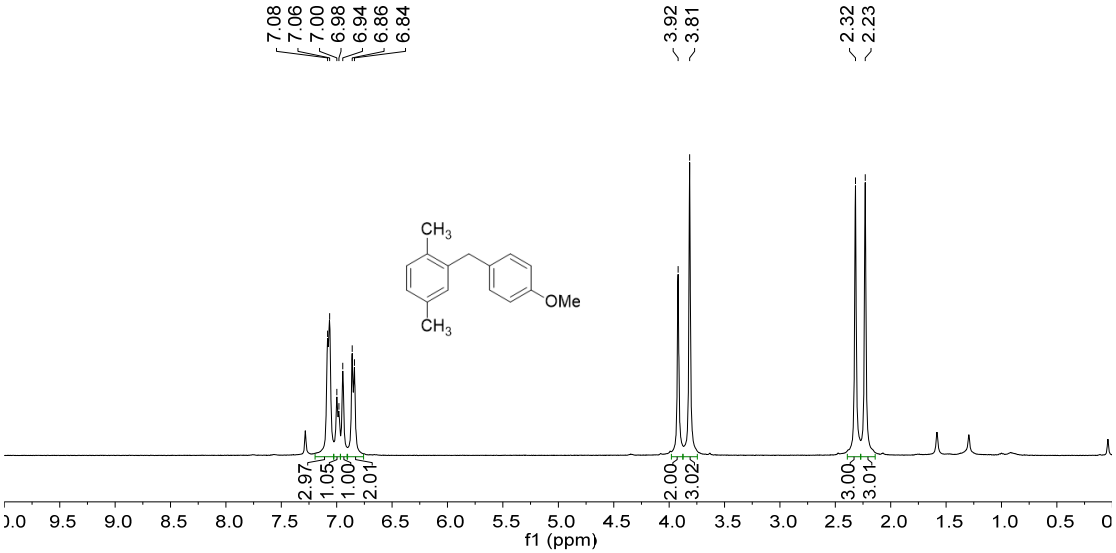

^{1}H NMR (400 MHz, $CDCl_3$) δ 7.20 – 7.03 (m, 3H), 6.99 (d, *J* = 7.8 Hz, 1H), 6.94 (s, 1H), 6.85 (d, *J* = 8.2 Hz, 2H), 3.92 (s, 2H), 3.81 (s, 3H), 2.31 (s, 3H), 2.23 (s, 3H).

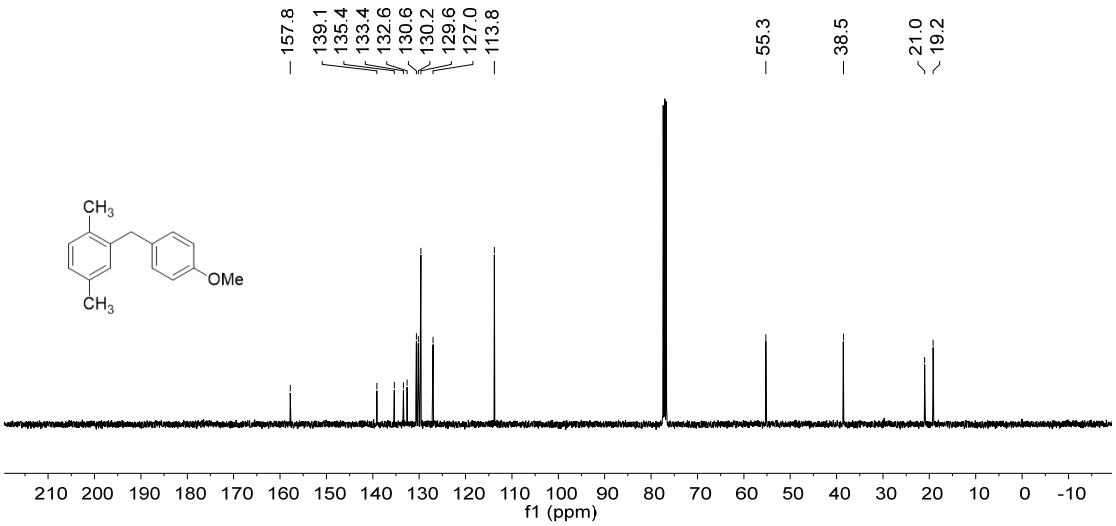

^{13}C NMR (100 MHz, $CDCl_3$) δ 157.8, 139.1, 135.4, 133.4, 132.6, 130.6, 130.2, 129.6, 127.0, 113.8, 55.3, 38.5, 21.0, 19.2.

22. Mass spectra data of the products

Diphenylmethane (Table 2, entry 1)

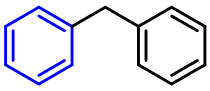

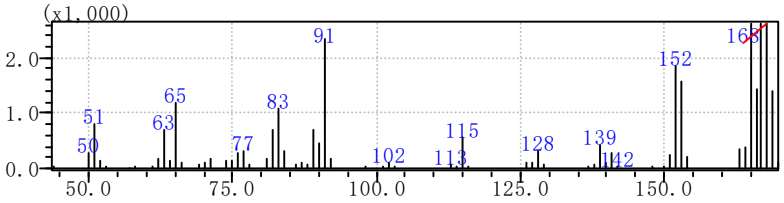

1,4-Dimethyl-2-(2-methylbenzyl)benzene (Table 2, entry 2)

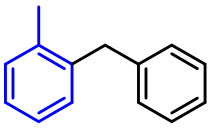

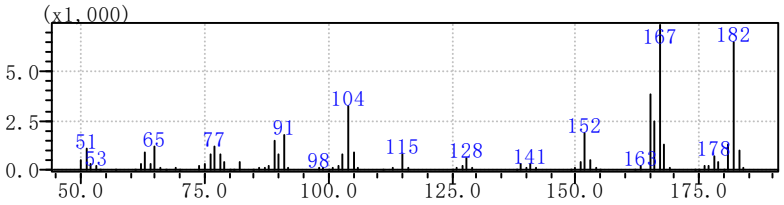

1-benzyl-2-ethylbenzene (Table 2, entry 3)

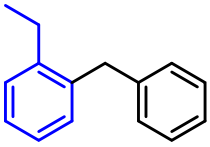

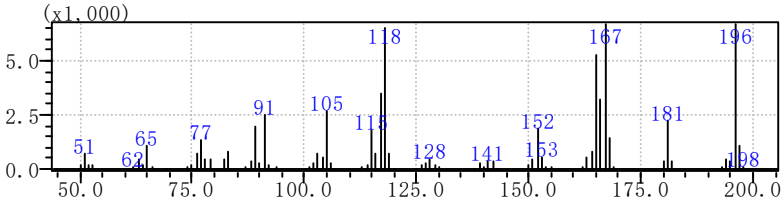

2-Benzyl-1,3,5-trimethylbenzene (Table 2, entry 4)

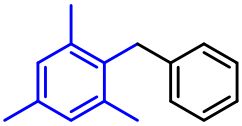

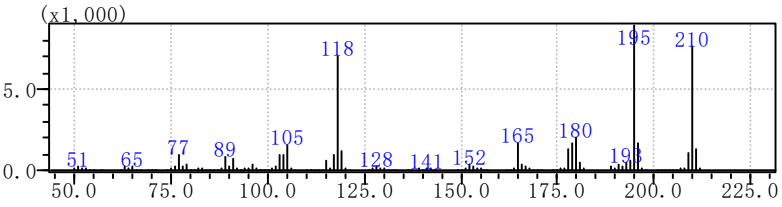

1-benzyl-2-methoxybenzene (Table 2, entry 5)

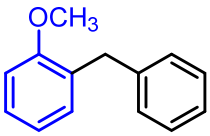

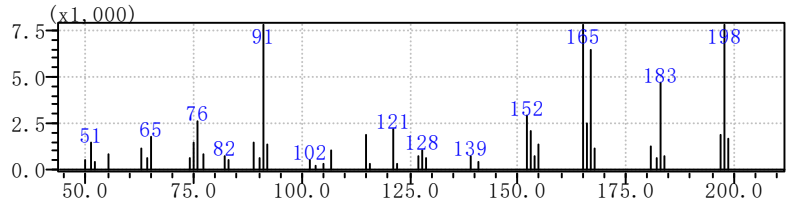

1-benzyl-2-isopropylbenzene (Table 2, entry 6)

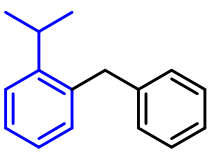

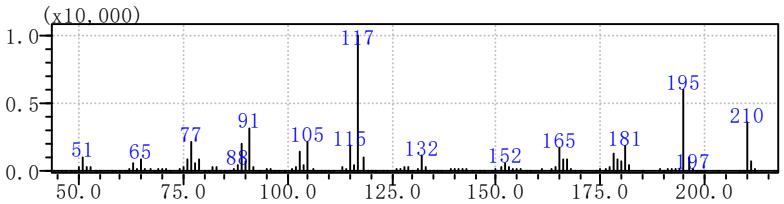

2-(2,5-Dimethylbenzyl)naphthalene (Table 2, entry 7)

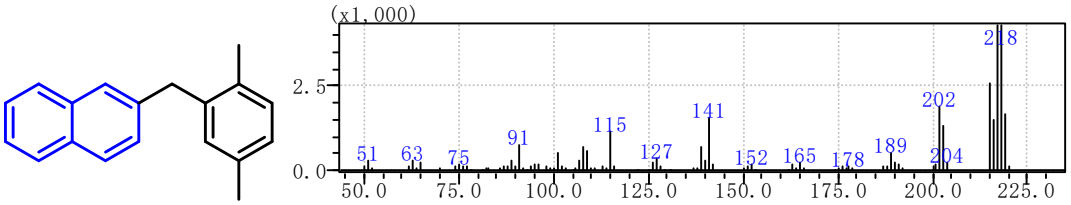

Methyl 4-(2,5-dimethylbenzyl)benzoate (Table 2, entry 8)

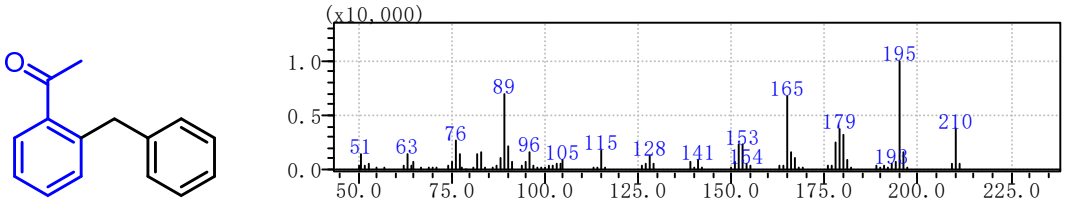

2-(1-chlorobenzyl)-1,4-dimethylbenzene (Table 2, entry 9)

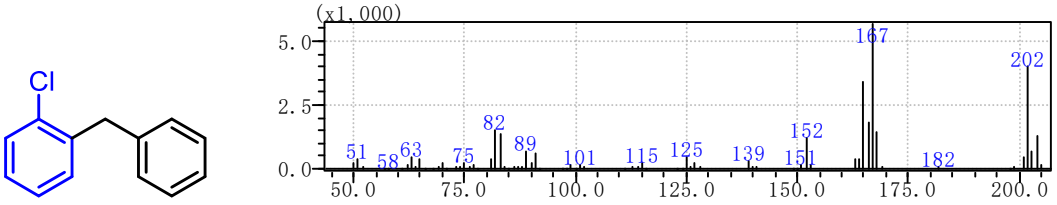

2-(1-Bromobenzyl)-1,4-dimethylbenzene (Table 2, entry 10)

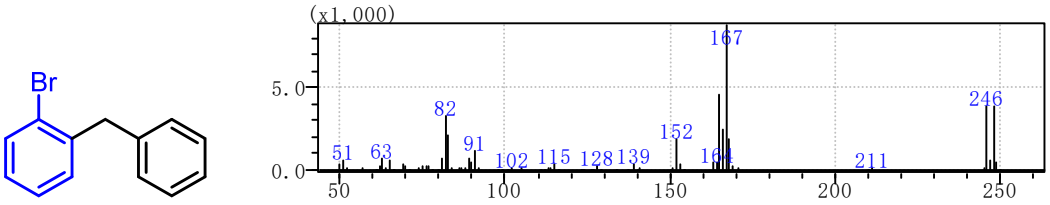

3-benzylpyridine (Table 2, entry 11)

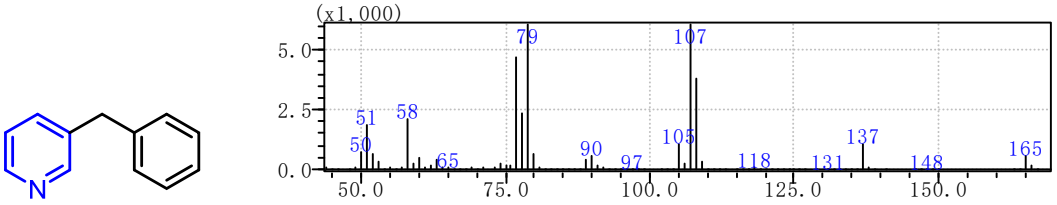

3-benzylquinoline (Table 2, entry 12)

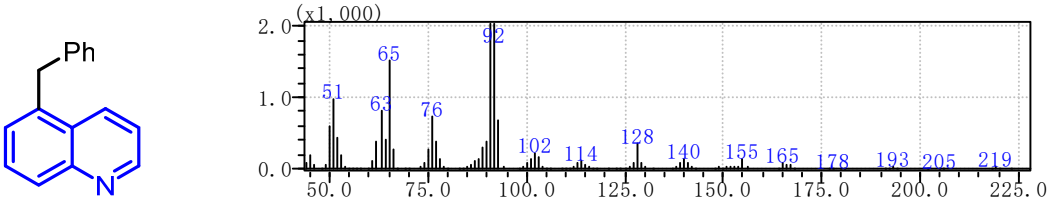

3-benzyl-1H-pyrrole (Scheme S4)

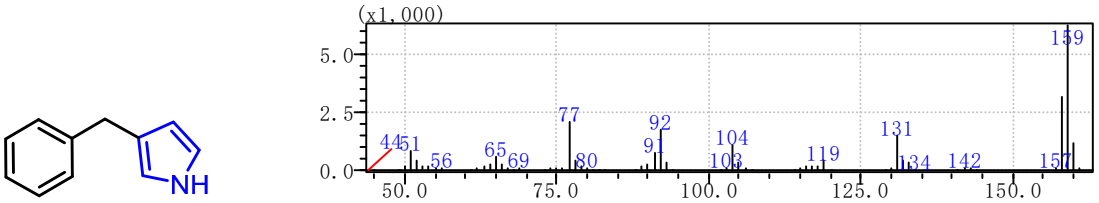

5-benzyl-1H-indole (Scheme S4)

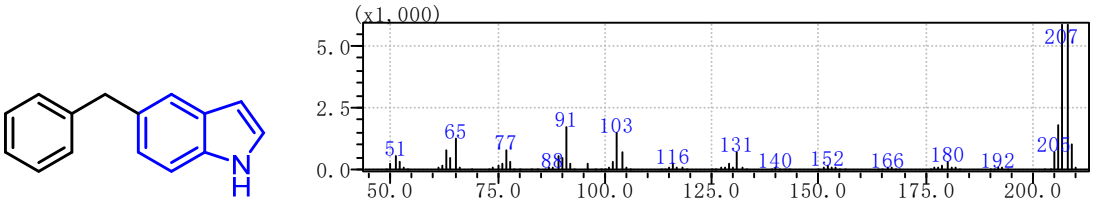

6-benzyl-2H-chromen-2-one (Table 2, entry 13)

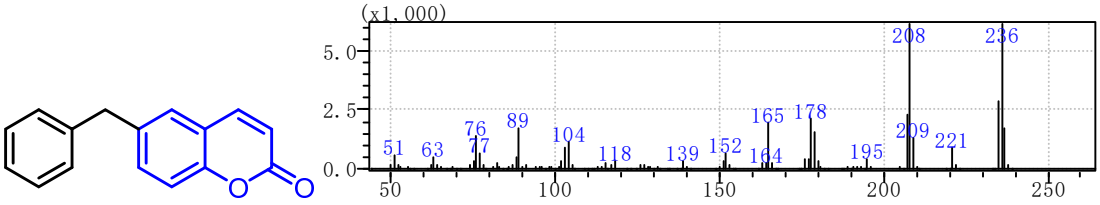

2-(4-chlorobenzyl)-1,4-dimethylbenzene (Table 2, entry 14)

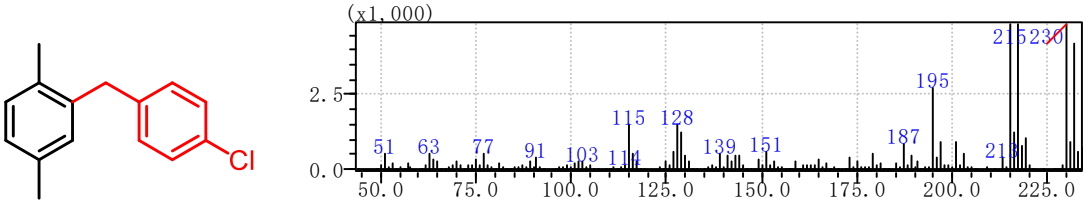

2-(4-bromobenzyl)-1,4-dimethylbenzene (Table 2, entry 15)

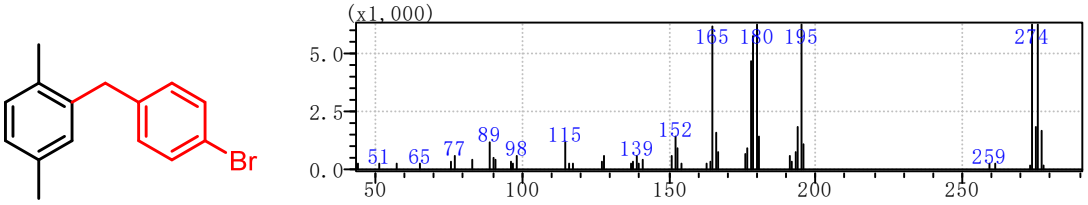

1,4-dimethyl-2-(4-methylbenzyl)benzene (Table 2, entry 16)

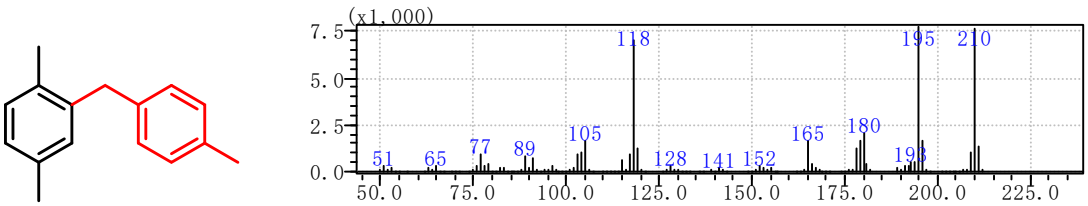

2-(4-methoxybenzyl)-1,4-dimethylbenzene (Table 2, entry 17)

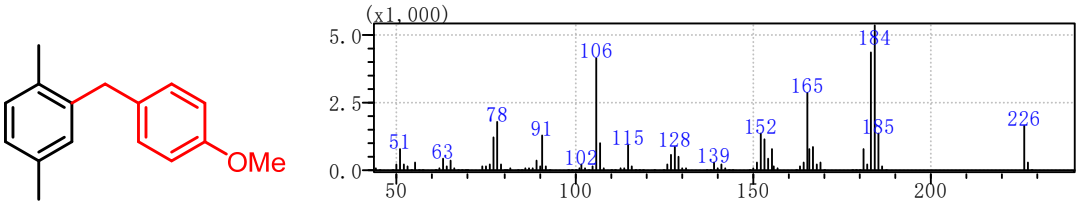

References

1. G. Kresse and J. Furthmuller, *Comp. Mater. Sci.*, 1996, **6**, 15-50.
2. G. Kresse and J. Furthmüller, *Phys. Rev. B*, 1996, **54**, 11169-11186.
3. J. P. Perdew, K. Burke and M. Ernzerhof, *Physical Review Letters*, 1996, **77**, 3865-3868.
4. G. Kresse and D. Joubert, *Phys. Rev. B*, 1999, **59**, 1758-1775.
5. P. E. Blöchl, *Physical Review B*, 1994, **50**, 17953-17979.
6. S. L. Dudarev, G. A. Botton, S. Y. Savrasov, C. J. Humphreys and A. P. Sutton, *Phys. Rev. B*, 1998, **57**, 1505-1509.
7. S. Grimme, J. Antony, S. Ehrlich and H. Krieg, *The Journal of chemical physics*, 2010, **132**, 154104.
8. B. Yuan, W. Zhao, F. Yu and C. Xie, *Catal. Commun.*, 2014, **57**, 89-93.
9. F. Wu, Y. Zhao, Y. Wang, Y. Xu, M. Tang, Z. Wang, B. Han and Z. Liu, *Green Chem.*, 2022, **24**, 3137-3142.
10. S. Zhang, X. Zhang, X. Ling, C. He, R. Huang, J. Pan, J. Li and Y. Xiong, *RSC Adv.*, 2014, **4**, 30768-30774.
11. P. A. Champagne, Y. Benhassine, J. Desroches and J.-F. Paquin, *Angew. Chem. Int. Ed.*, 2014, **53**, 13835-13839.
12. M. Kaneko, R. Hayashi and G. R. Cook, *Tetrahedron Lett.*, 2007, **48**, 7085-7087.
13. M. Ramos-Martín, J. García-Álvarez and A. P. Soto, *ChemSusChem*, 2025, **18**, e202400892.
14. C. Y. Zhang, X. Q. Gao, J. H. Zhang and X. J. Peng, *Chin. Chem. Lett.*, 2009, **20**, 913-916.
15. P. Moriel and A. B. García, *Green Chem.*, 2014, **16**, 4306-4311.
16. T. He, H. F. T. Klare and M. Oestreich, *ACS Catal.*, 2021, **11**, 12186-12193.
17. T. Mukaiyama, M. Ueki, T. Izawa and M. Kuwahara, *Chem Lett*, 2006, **1**, 443-444.
18. B.-Q. Wang, S.-K. Xiang, Z.-P. Sun, B.-T. Guan, P. Hu, K.-Q. Zhao and Z.-J. Shi, *Tetrahedron Lett.*, 2008, **49**, 4310-4312.
19. T. Tsuchimoto, K. Tobita, T. Hiyama and S.-i. Fukuzawa, *J. Org. Chem.*, 1997, **62**, 6997-7005.
20. I. Shiina and M. Suzuki, *Tetrahedron Lett.*, 2002, **43**, 6391-6394.
21. K. Mertins, I. Iovel, J. Kischel, A. Zapf and M. Beller, *Angew. Chem. Int. Ed.*, 2005, **44**, 238-242.
22. S. Podder and S. Roy, *Tetrahedron*, 2007, **63**, 9146-9152.
23. R. M. N. Kalla, R. Chakali, M. Amudala, M. Varalakshmi and C. Nagaraju, *Organic Communications*, 2021, DOI: 10.25135/acg.oc.106.2104.2034, 300-304.
24. B. Yuan, Y. Li, Z. Wang, F. Yu, C. Xie and S. Yu, *Molecular Catalysis*, 2017, **443**, 110-116.
25. Y. Wang, Y. Y. Sun, C. Lancelot, C. Lamonier, J. C. Morin, B. Revel, L. Delevoye and A. Rives, *Microporous and Mesoporous Materials*, 2015, **206**, 42-51.
26. N. N. Karade, S. G. Shirodkar and R. A. Potrekar, *J Chem Res*, 2003, 652-654.

27. M. H. Al-Hazmi and A. W. Apblett, *Catal. Sci. Technol.*, 2011, **1**, 621-630.
28. J. R. Satam and R. V. Jayaram, *Catal. Commun.*, 2008, **9**, 1937-1940.
29. T. Lin, X. Zhang, R. Li, T. Bai and S. Y. Yang, *Chin. Chem. Lett.*, 2011, **22**, 639-642.
30. J. Li, Y. Zhou, D. Mao, G. Chen, X. Wang, X. Yang, M. Wang, L. Peng and J. Wang, *Chem. Eng. J.*, 2014, **254**, 54-62.
31. C. Khatri, M. K. Mishra and A. Rani, *Fuel Processing Technology*, 2010, **91**, 1288-1295.
32. Y. Rao, M. Trudeau and D. Antonelli, *J. Am. Chem. Soc.*, 2006, **128**, 13996-13997.
33. C. Ramesh Kumar, K. T. V. Rao, P. S. Sai Prasad and N. Lingaiah, *J. Mol. Catal. A: Chem.*, 2011, **337**, 17-24.
34. F. Wang and W. Ueda, *Chem. Eur. J.*, 2009, **15**, 742-753.
35. S. Pan, J. Liu, Y. Li and Z. Li, *Chin. Sci. Bull.*, 2012, **57**, 2382-2386.
36. P. Xiang, K. Sun, S. Wang, X. Chen, L. Qu and B. Yu, *Chin. Chem. Lett.*, 2022, **33**, 5074-5079.
37. J.-C. Hou, J. Jiang, H. Dai, J.-S. Wang, T. Li, X. Chen and W.-M. He, *Science China Chemistry*, 2025, **68**, 1945-1951.
38. X. Du, C. Zhang and S. Liu, *Dalton Trans.*, 2022, **51**, 15322–15329.